On the Right Track?
Designing Optimal Public Transit Contracts

Matías Navarro*
Cornell University

Job Market Paper | November 22, 2025

Please click here for the latest version

Abstract

Private transit provision faces two opposing market failures: market power, which leads firms to set high prices and underprovide quality, and uninternalized network effects that arise from fragmented service and lack of coordination across routes. Governments address these distortions through contracts that combine quality targets with route bundling. This paper studies how these instruments should be designed to maximize welfare. I exploit quasi-experimental variation from Santiago, Chile's 2022 contract reform which imposed stricter quality targets and rebundled routes among private operators. Using high-frequency GPS data for 373 bus routes and an event-study difference-in-differences design, I find that stricter quality targets improve service regularity by 16 percent and increase ridership by 7.5 percent. I develop and estimate a structural model that endogenizes traveler mode and route choices, private operators' service attribute decisions, and traffic congestion to evaluate alternative contract designs. The results show that welfare losses from monopoly pricing exceed coordination gains from single-operator networks, with optimal market structure involving four to five competing firms. The findings highlight that effective contract design must reconcile the efficiency gains from competition with the coordination benefits of network integration.

Keywords: Public Transit. Private Provision. Contracts. Network Effects. JEL: D22, D62, L91, L92, R41, R42

*Dyson School of Applied Economics and Management, Cornell University (Email: min26@cornell.edu.).
I am grateful to my advisors Shanjun Li, Todd Gerarden, Andrew Waxman, and Stuart Rosenthal for invaluable advice and support, and to Ricardo Daziano, Seba Tamblay, Beia Spiller, and seminar participants at Cornell University, AERE Summer Conference, ITEA Annual Conference for helpful comments. I gratefully acknowledge support by the Interdisciplinary Transportation Doctoral Fellowship funded by the Alfred P. Sloan Foundation. All errors are mine.

1 Introduction

Governments often rely on private firms to deliver public services, with procurement accounting for roughly 12% of global GDP (Bosio *et al.*, 2022; Wolfram *et al.*, 2023). Procurement outcomes depend critically on how contracts allocate risks and incentives, especially when multiple market failures coexist (Lewis and Bajari, 2014). In this sense, procurement contract design involves a fundamental trade-off: instruments that curb one source of inefficiency may exacerbate another. This trade-off arises across many sectors, and is particularly salient in network industries such as energy distribution, broadband, water utilities, and public transit. In transit markets, economic theory predicts two coexisting market failures. The first is market power, which leads to inefficient prices and underprovision of quality by ignoring the environmental benefits of mode shift from cars to transit (Spence, 1975). The second is uninternalized network effects, whereby firms coordinate within their own routes but neglect complementarities across routes operated by other firms (Economides, 1996).

In recent decades, transit agencies have increasingly relied on contractual mechanisms to regulate service provision, with mixed results (e.g., Paris, Singapore, Hong Kong; see Figure C.1). Among the many dimensions of contract design, two are central because they directly target the market failures described above. The first is quality targets, which discipline firm behavior by imposing minimum service standards. They mitigate the underprovision that results from market power but raise operating costs and, in turn, the subsidies or prices needed to sustain service. The second is route bundling, which determines how many routes are grouped within a single contract. Smaller bundles expand the pool of potential operators and reduce the price distortions of market power, but they fragment the network and weaken coordination. Larger bundles preserve coordination across routes but reduce competition. Each instrument therefore addresses one dimension of inefficiency while potentially worsening the other. What remains unclear, and is central for contract design, is how these instruments interact when both market power and network effects are present.

In this paper, I study how quality targets and route bundling should be designed in public transit contracts to maximize welfare. I study this question in the context of Santiago de Chile's public transit system, Transantiago, one of the first large-scale systems to adopt contracts regulating private bus service. These contracts group routes into packages operated by private firms, compensate firms for service provision, and specify targets on service attributes. Each year, Transantiago pays roughly $900 million to these private operators to run 373 bus routes that, together with the subway network, serve approximately 2.6 million trips per day. In late 2022, a large-scale contract reform modified both the stringency of quality targets and the number of route bundles, affecting over 40

percent of the network. This reform provides a unique setting to test how contract design can address market power and network effects.

I begin by analyzing the market failures in private provision of public transit using a framework adapted from Barwick *et al.* (2024a). In the baseline model, a monopolist and a social planner each choose prices and service attributes. I extend this framework by allowing travelers' willingness to pay on one route to depend on service quality elsewhere in the network. This captures demand-side network effects.

The conceptual framework highlights two distortions. The first is market power, which induces firms to charge markups and underprovide quality, given that they do not internalize the environmental benefits of shifting travelers from cars to transit. The second is uninternalized network effects, as firms coordinate service within their own routes but neglect complementarities across routes operated by others. These distortions motivate two contractual instruments. Quality targets can discipline service provision, but their welfare effect depends on how penalties are designed: they restore efficiency if they internalize the value of the environmental benefits, yet they may also raise costs and fares. Route bundling can mitigate markups by fostering competition, but it fragments the network and weakens coordination across routes.

The interaction of these instruments is even less clear. Stricter quality targets increase operating costs, which may amplify the effects of market power if competition is weak. Conversely, smaller bundles intensify competition but may reduce the effectiveness of quality targets if coordination breaks down. Theory therefore delivers sharp predictions about the sources of inefficiency but leaves ambiguous how contract instruments should be designed jointly. This ambiguity motivates the empirical analysis.

In the empirical analysis, I draw on rich administrative data that directly connect traveler choices to the service they experience. I combine (i) a representative household travel survey that records not only precise trip origins and destinations but also travelers' mode and route choices, (ii) the universe of smart-card fare validations, which reconstructs complete journeys including transfers, and (iii) GPS signals from every transit vehicle, emitted every 30 seconds. Together, these sources provide a unique match between demand and supply: I observe which routes travelers choose and, conditional on that choice, the exact service attributes they encounter such as fares, travel times, frequency, and regularity of service.

I use these data to provide descriptive evidence on two central mechanisms behind the contract reform. First, I study the effect of quality targets on service attribute choices. Using raw data, I show that firms consistently meet frequency targets but fall short of regularity targets. This divergence is informative: it indicates that the marginal cost of improving regularity exceeds the expected penalties, so firms rationally allocate effort across attributes rather than complying uniformly. To go beyond this descriptive evidence, I

exploit the 2022 contract reform, which introduced stricter quality targets on 40 percent of routes. This reform functions as a natural experiment in enforcement because it creates counterfactual regimes within the same market, something rarely observed in public procurement. Using a difference-in-differences design, I show that stricter quality targets shift behavior: regularity increases by about 16 percent, consistent with firms reoptimizing in response to stronger enforcement. Frequency rises by only 2.9 percent and the estimate is not statistically significant, which aligns with the fact that firms were already meeting frequency targets. These adjustments reduce waiting times and improve service quality. Finally, I show that travelers respond to these improvements: ridership rises by 7.5 percent on routes subject to stricter quality targets relative to those that were not. Together, these results provide direct evidence on how contract design affects both firm behavior and demand.

Second, I examine the effect of network fragmentation on service attributes, focusing on the second policy change introduced in the 2022 contract reform: the creation of more route bundles. Bundling determines how many firms operate within a market, and in turn how fragmented the network is. I use the household travel survey to define markets as origin destination zone pairs and track daily service attributes over time. I measure network fragmentation with a standard index of market concentration, the Herfindahl Hirschman Index (HHI), and relate it to frequency, headway regularity, and wait times. Three patterns emerge. First, frequency declines with concentration: as HHI rises, firms deploy fewer buses, consistent with under provision driven by market power. Second, regularity improves with concentration: the coefficient of variation of headways falls as HHI rises, consistent with firms better coordinating dispatches when they control all routes in a market. Third, wait times fall modestly with concentration, indicating that the coordination effect slightly outweighs the quantity effect. These results show that bundling routes alters the structure of competition in ways that reduce frequency but improve regularity, with overall waiting times determined by the balance of market power and coordination forces.

These findings suggest that quality targets and network fragmentation shape service provision and traveler responses in meaningful ways. They also highlight trade-offs that cannot be assessed with reduced-form evidence alone: how operator costs respond to stricter quality targets or to bundling that alters market structure, how these policy instruments interact in shaping supply and demand, and what the welfare consequences are under alternative designs.

I develop and estimate a model of public transportation outsourcing to analyze these trade-offs. The model has three components. On the demand side, I estimate traveler preferences from revealed mode and route choices. On the supply side, I estimate operator cost parameters from service attribute choices using the identifying variation generated

by the 2022 contract reform. Finally, a road technology component links traffic flows to equilibrium travel times in the road network.

On the demand side, I estimate travel preference parameters for in-vehicle travel time, wait time, fares, and transfer penalties using maximum likelihood estimation of travelers' mode and route choices, following Kreindler *et al.* (2023). The demand side of the model captures complementarities across routes and the welfare gains from quality improvements. On the supply side, I estimate operator cost parameters from firms' profit-maximizing first-order conditions to identify labor elasticity, quality elasticity, and economies-of-scale parameters. The supply side of the model captures the trade-offs firms face in meeting stricter quality targets and the efficiency gains that can arise from bundling. On the road technology side, I estimate a congestion elasticity parameter using traffic counts and speed data at 64 locations in the city. The road technology component reproduces equilibrium travel times in the road network and captures how congestion responds to traveler and operator choices.

The estimated model aligns closely with the descriptive evidence. On the demand side, the marginal disutility of waiting is about 1.8 times that of in-vehicle travel, the implied value of time is near $11 per hour, and there is a sizable transfer penalty. On the supply side, the estimates reveal sharp asymmetries in adjustment costs: a 10 percent increase in frequency raises operating costs by roughly 6.4 percent, whereas a 10 percent improvement in regularity increases costs by about 11.4 percent. Operating costs also fall by about 2.2 percent when more routes operate from the same depot, indicating modest economies of scale at the depot level. On the road technology side, the elasticity of travel time with respect to traffic flows is about 0.12, which is comparable to existing estimates in the literature (Akbar *et al.*, 2023). The model reproduces key outcomes in the data, explaining 56 percent of the variation in route-level ridership and 12 percent of the variation in speeds. These magnitudes rationalize the reduced-form findings: regularity is more costly to improve than frequency, consistent with firms deviating more on that margin before the reform. The model therefore provides a disciplined foundation for evaluating the welfare implications of alternative quality targets and route bundling.

Using these estimates, I first examine how market structure affects welfare in the absence of regulation. A monopoly sets higher fares and underprovides quality, but coordinates operations across the entire network. Adding more firms introduces competition on prices but fragments the network, which increases environmental externalities. I find that consumer surplus rises only modestly and producer surplus falls only gradually as the number of firms grows. This pattern reflects an important nuance: because the bundles I simulate isolate firms in nearly disjoint geographic areas, competition does not fully materialize, and each firm retains local market power. As a result, prices do not decline as much as theory might predict, and externalities from fragmentation eventually dominate,

lowering welfare at higher levels of competition.

I then evaluate the performance of quality targets, which represent the main regulatory tool currently in place. These targets penalize firms for underperforming on service attributes and can, in theory, push provision closer to the social optimum. In my simulations, quality targets substantially reduce externalities and improve passenger experience, but they do not alter firms' ability to charge prices above cost. The outcome resembles a set of local monopolies that are disciplined on quality but not on prices, so welfare improves relative to the unregulated case but remains far from the planner's benchmark.

Finally, I consider the role of route bundling, which determines how competition unfolds. The current bundling design generates local monopolies that limit the effectiveness of competition, which explains why producer surplus remains high even as more firms enter. My framework suggests that alternative bundling strategies—by mixing routes across geographic areas—could enhance competition and reduce local market power. Importantly, this policy would complement quality targets by addressing different market failures: bundling would discipline prices, while targets would discipline quality. Together, they have the potential to bring market outcomes much closer to the social planner's benchmark, though the design must balance stronger competition against the risk of further fragmentation.

Related literature This paper contributes to the growing literature on the design and evaluation of public transit policies. One line of research has examined settings where provision is largely public and centralized, focusing on policies such as price, subsidy, and service-attribute design (Parry and Small, 2009; Wang, 2024), congestion pricing (Barwick *et al.*, 2024b; Almagro *et al.*, 2022), and transit infrastructure and network design (Tsivanidis, 2025; Kreindler *et al.*, 2023). A second line has studied decentralized private provision, emphasizing the externalities of unregulated markets, including matching (Conwell, 2023), safety (Kelley *et al.*, 2024), market segmentation (Mbonu and Eaglin, 2024), and public entry (Björkegren *et al.*, 2025). A smaller but important set of papers investigates regulated private operators, including work using structural models to study regulatory schemes or the strategic organization of depots and routes (e.g., Gagnepain and Ivaldi, 2002; Marra and Oswald, 2023). My paper is complementary to this work: I focus on how contract design, through explicit instruments such as quality targets and route bundling, reshapes firms' incentives in ways that matter for service quality, passenger behavior, and overall welfare, highlighting its importance as a core policy instrument in public transit.

The paper also relates to the broader literature on private participation in the provision of public services. A large body of work has examined how privatization and outsourcing affect efficiency, quality, and access in sectors such as water, electricity, and health, with

evidence ranging from water utilities (Galiani *et al.*, 2005) to hospitals (Duggan, 2000). This literature highlights the challenges of incomplete contracts and limited monitoring, which can lead to cost savings at the expense of quality (Hart *et al.*, 1997; Levin and Tadelis, 2010; Bajari and Tadelis, 2001). Empirical studies document both the efficiency gains and the risks of quality shading under private provision, with evidence from procurement in municipal services (Jerch *et al.*, 2017), water and electricity utilities, and infrastructure (Lewis and Bajari, 2011, 2014; Bajari *et al.*, 2014). A central theme in this research is the tension between harnessing competition and safeguarding service quality when performance is difficult to specify or enforce. My analysis contributes to this debate by leveraging quasi-experimental variation from a major contract reform in Santiago, where stricter quality targets and route rebundling were introduced on only 40 percent of routes. This staggered and partial implementation generates clean policy variation, allowing me to provide direct evidence on how contractual instruments shape service provision. Together, these findings highlight the central role of contract design in determining quality outcomes in outsourced public services.

Finally, this paper builds on the use of structural models to study transportation industries. Recent work has applied such approaches to analyze spatial equilibrium and platform competition in taxi and ride-hailing markets (Buchholz, 2022; Frechette *et al.*, 2019; Castillo, 2025; Rosaia, 2025), search frictions and optimal policy in decentralized transport markets (Brancaccio *et al.*, 2023), and the role of shipping networks in world trade (Brancaccio *et al.*, 2020). Other studies have examined network competition and economies of scope in railroads and airlines (Chen, 2024; Degiovanni and Yang, 2023; Ciliberto *et al.*, 2021; Yuan and Barwick, 2024), and AI-assisted decision-making in trucking maintenance (Harris and Yellen, 2024). These studies demonstrate how structural models can uncover the welfare consequences of regulation and market structure in settings where firm behavior interacts with infrastructure. My contribution is to extend this framework to regulated urban bus transit, where contracting, rather than direct pricing, is the central policy instrument. In particular, I use the model to study the interaction between quality targets and route rebundling—two instruments that address different aspects of market power and network effects, but whose joint impact is theoretically ambiguous. The contract reform generates quasi-experimental variation in quality targets and route rebundling that reveals how firms adjust frequency and service regularity when incentives shift. This identifying variation pins down key supply-side elasticities in the cost function, which determine how firms would reoptimize service attributes under alternative contract designs. As a result, the model can generate credible counterfactuals that quantify the welfare implications of contract design in urban bus transit and offer insights for the regulation of networked service industries more broadly.

2 Theoretical Framework

In this section, I present a theoretical framework for optimal regulation of transit service provision in the presence of market power, environmental externalities, and network effects. As a key departure from the literature on transportation regulation under market power, firms in this model respond to government policies by adjusting both prices and service attributes of their route networks. This framework enables me to characterize the welfare implications of two policy instruments: quality targets and route bundling.

The framework involves N differentiated transit routes, indexed by j, each characterized by a K-element service attribute vector $x_j = (x_j^1, x_j^2, \ldots, x_j^K)$ (e.g., frequency, headway regularity) and price P_j. Route j generates external benefits $e_j(x_j) > 0$ due to reductions in pollution and traffic congestion externalities when travelers shift from more externality-intensive transportation modes. Both consumer willingness-to-pay $B_j(x)$ and the marginal cost of service provision $C_j(x_j)$ depend on service attributes, where $x = (x_1, \ldots, x_N)$ captures network effects arising from the interdependence of route choices.

Throughout the theoretical analysis, I assume that consumer demand exhibits additive separability between price disutility and service attributes: $Q_j(P, x) = Q_j\left(P_j - B_j(x)\right)$. following Barwick *et al.* (2024a). The additive separability makes firms' choices of prices and attributes independent and greatly simplifies the model. Most importantly, it enables me to characterize optimal policy design in the presence of market power and network externalities, which has not been done in the transit regulation literature. A limitation of the additivity assumption is that the marginal value of service attributes is the same across consumers, which rules out the Spence distortion in quality provision.

The theoretical analysis compares the privately and socially optimal outcomes and discusses the choice of regulatory instruments to rectify market failures in transit provision. To build intuition, I first analyze the baseline case of a social planner before examining monopoly provision without regulation, then extending to quality regulation and competitive bundling mechanisms.

2.1 Social Planner

The social planner chooses prices and service attributes to maximize social welfare that consists of consumer surplus, producer surplus, and externalities.

$$\max_{P,x} \quad SW(P,x) = \sum_{j=1}^{N} \Bigg[\underbrace{\int_0^{Q_j(P,x)} \Big(B_j(x) + Q_j^{-1}(s) - P_j \Big)\, ds}_{\text{Consumer surplus}} + \underbrace{\big(P_j - C_j(x_j)\big)\, Q_j(P,x)}_{\text{Producer surplus}} + \underbrace{\phi \cdot e_j(x_j) Q_j(P,x)}_{\text{Externality}} \Bigg]$$

The socially optimal prices P_j^* and service attributes x_j^* satisfy the following first-order conditions:

$$[P_j]: \quad P_j^* - C_j(x_j^*) + \phi \cdot e_j(x_j^*) = 0 \tag{1}$$

$$[x_\ell^i]: \quad \underbrace{\left[\frac{\partial B_i(x^*)}{\partial x_\ell^i} - \frac{\partial C_i(x_i^*)}{\partial x_\ell^i} + \phi \cdot \frac{\partial e_i(x_i^*)}{\partial x_\ell^i} \right] Q_i}_{\text{Direct effect on route } i} + \underbrace{\sum_{j \neq i}^{N} \left[\frac{\partial B_j(x^*)}{\partial x_\ell^i} Q_j \right]}_{\text{Network effect}} = 0 \tag{2}$$

The first-order conditions reflect that service attributes are chosen to maximize per-unit social surplus, $B_j(x) - C_j(x_j) + \phi \cdot e_j(x_j)$, while prices reflect the social cost of service provision, $C_j(x_j^*) - \phi \cdot e_j(x_j^*)$. The socially optimal price P_j^* eliminates quantity distortions, while the socially optimal attributes x_j^* internalize both environmental externalities and network effects across routes.

2.2 Monopoly without Regulation

Consider a monopolist that controls the entire transit network and chooses prices and service attributes to maximize profit:

$$\max_{P,x} \quad \Pi(P,x) = \sum_{j=1}^{N} \left[\big(P_j - C_j(x_j)\big)\, Q_j(P,x) \right]$$

The privately optimal prices P_j^m and service attributes x_j^o satisfy:

$$[P_j]: \quad \frac{P_j^m - C_j(x_j^o)}{P_j^m} = \frac{1}{\varepsilon_{P_j}}$$

$$[x_\ell^i]: \quad \underbrace{\left[\frac{\partial B_i(x^o)}{\partial x_\ell^i} - \frac{\partial C_i(x_i^o)}{\partial x_\ell^i}\right] Q_i}_{\text{Direct effect on route } i} + \underbrace{\sum_{j \neq i}^{N} \left[\frac{\partial B_j(x^o)}{\partial x_\ell^i} Q_j\right]}_{\text{Network effect}} = 0$$

where ε_{P_j} is the price elasticity of demand for route j. The first-order conditions differ from Equations (1) and (2) in three important ways.

First, the monopolist sets $P_j^m > P_j^*$, resulting in underprovision of quantity relative to the social optimum due to markup pricing under downward-sloping demand. Second, the monopolist does not internalize external benefits $\phi \cdot e_j(x_j)$, leading to inefficient service quality choices where routes may be under-served in terms of environmentally beneficial attributes. Third, while the monopolist controls all routes and thus internalizes network effects through the term $\sum_{j \neq i} \frac{\partial B_j(x^o)}{\partial x_\ell^i} Q_j$, it chooses suboptimal attribute levels because it ignores externalities. Consequently, it does not generate the full social value of network coordination that would justify higher service levels.

2.3 Monopoly with Quality Regulation

Suppose the government introduces quality targets $\bar{x}_j$ for each route j to address externality distortions. To incentivize compliance, the firm faces penalties when deviating from these targets:

$$\mathcal{P}_j(x_j, \bar{x}_j) = \tau \cdot s_j(x_j, \bar{x}_j),$$

where $\tau > 0$ is a penalty strength parameter and $s_j(\cdot)$ represents the penalty function. The regulated monopolist maximizes:

$$\max_{P,x} \quad \Pi(P, x) = \sum_{j=1}^{N} \left[\left(P_j - C_j(x_j) - \tau \cdot s_j(x_j, \bar{x}_j)\right) Q_j(P, x)\right]$$

The regulated equilibrium prices P_j^z and service attributes x_j^z satisfy:

$$[P_j]: \quad \frac{P_j^z - C_j(x_j^z) - \tau \cdot s_j(x_j^z, \bar{x}_j)}{P_j^z} = \frac{1}{\varepsilon_{P_j}}$$

$$[x_\ell^i]: \quad \underbrace{\left[\frac{\partial B_i(x^z)}{\partial x_\ell^i} - \frac{\partial C_i(x_i^z)}{\partial x_\ell^i} - \tau \cdot \frac{\partial s_i(x_i^z, \bar{x}_i)}{\partial x_\ell^i}\right] Q_i}_{\text{Direct effect on route } i} + \underbrace{\sum_{j \neq i}^{N} \left[\frac{\partial B_j(x^z)}{\partial x_\ell^i} Q_j\right]}_{\text{Network effect}} = 0$$

Quality regulation addresses externality distortions but leaves market power intact. The monopolist continues to set $P_j^z > P_j^*$, leading to underprovision of quantity relative to the social optimum, as the penalty function affects profit levels but not marginal pricing incentives. However, if the marginal penalty equals the marginal externality:

$$\tau \cdot \frac{\partial s_j(x_j, \bar{x}_j)}{\partial x_\ell^j} = \phi \cdot \frac{\partial e_j(x_j)}{\partial x_\ell^j} \quad \text{for all } j, \ell,$$

then the regulated monopolist chooses efficient service quality levels: $x_j^z = x_j^*$. Under this condition, the monopolist also internalizes the full network benefits that a social planner would, since it controls all routes and quality incentives are properly aligned.

2.4 Competitive Route Bundling

I now introduce a two-stage mechanism where competition occurs via auctions over packages of transit routes, followed by decentralized service provision by winning firms. This mechanism addresses market power distortions while potentially affecting the internalization of network effects.

The N transit routes are partitioned into B disjoint packages $\mathcal{R}_b \subset \{1, \ldots, N\}$. In the first stage, firms $k \in \mathcal{K}$ submit bids P_{kb} representing the per-passenger price they would charge for operating bundle b. The regulator awards each bundle to the lowest bidder:

$$k(b) = \arg\min_{k \in \mathcal{K}} P_{kb}.$$

In the second stage, each winning firm chooses service attributes x_j for routes $j \in \mathcal{R}_b$ to maximize profit, taking prices as given from the auction outcome.

2.4.1 First-Stage Bidding

In the auction stage, firm k chooses bid P for bundle b to maximize expected profit. Assuming symmetric firms with i.i.d. rival bids following distribution $F(\cdot)$, the probability of winning with bid P is $(1 - F(P))^{n-1}$, where n is the number of bidders. Expected profit is:

$$\max_P \quad (1 - F(P))^{n-1} \cdot \pi_k(P),$$

where $\pi_k(P) = \sum_{j \in \mathcal{R}_b} \left(P - C_j(x_j^{auction}) \right) Q_j$.

The first-order condition for optimal bidding yields:

$$\sum_{j \in \mathcal{R}_b} \left[(P_b - C_j(x_j^{auction})) \cdot \frac{\partial Q_j}{\partial P} + Q_j \right] = (n-1) \cdot \pi_k(P_b) \cdot \frac{f(P_b)}{1 - F(P_b)}$$

This condition balances the marginal profit from raising the bid (left side) against the increased probability of losing the auction (right side). As competition intensifies (n increases), the equilibrium bid P_b decreases toward marginal cost, addressing the quantity distortion from market power.

2.4.2 Second-Stage Service Provision

After winning bundle b, firm k chooses service attributes to maximize profit given the auction-determined price P_b:

$$\max_{x_j : j \in \mathcal{R}_b} \sum_{j \in \mathcal{R}_b} \left[\left(P_b - C_j(x_j) \right) \cdot Q_j(P_b, x) \right].$$

The optimal service attributes satisfy:

$$[x_\ell^i]: \quad \underbrace{\left[\frac{\partial B_i(x^{auction})}{\partial x_\ell^i} - \frac{\partial C_i(x_i^{auction})}{\partial x_\ell^i} \right] Q_i}_{\text{Direct effect on route } i} + \underbrace{\sum_{j \in \mathcal{R}_b, j \neq i} \left[\frac{\partial B_j(x^{auction})}{\partial x_\ell^i} Q_j \right]}_{\text{Within-bundle network effect}} = 0 \tag{3}$$

Comparing Equation (3) with (2) reveals that competitive bundling internalizes network effects only within each bundle $\mathcal{R}_b$, but not across bundles operated by different firms. The mechanism eliminates externality distortions only if combined with appropriate quality regulation, and the efficiency of network effect internalization depends critically on how routes are grouped into bundles.

2.5 Discussion

My theoretical framework illustrates the distinct roles of quality regulation and competitive bundling in addressing market failures in transit provision. Quality targets can eliminate externality distortions and restore efficient network coordination when properly calibrated, but leave market power intact. Competitive bundling addresses market power through price competition but may fragment network coordination depending on bundle design. The optimal regulatory approach depends on the relative importance of these distortions and the administrative feasibility of different policy instruments, questions I address empirically in the next sections.

3 Background and Institutional Setting

My empirical setting is Santiago's public transit system, Transantiago, administered by the *Directorio de Transporte Público Metropolitano* (DTPM), the public agency responsible for planning, contracting, and monitoring private bus operations. Since its launch in 2007, Transantiago has delegated operation of its 373 routes, served by a fleet of 6,982 buses, to private firms through competitively tendered contracts, while the metro network remains publicly operated. The two modes are fare-integrated, enabling seamless travel across the system.[1] In 2022, the system served an average of 2.6 million daily trips on business days, accounting for about 22 percent of total trips in the metropolitan area (CEDEUS, 2024). The total system budget reached US$1.35 billion (DTPM, 2022), of which US$900 million (67 percent) was allocated to payments to private operators, placing Transantiago among the ten largest public expenditure programs in Chile, alongside national initiatives in education, pensions, and housing (DIPRES, 2022). Transantiago is one of the most mature and extensive examples of contract-based bus regulation worldwide, typifying the "regulated competition" model now adopted in cities such as Singapore, Paris, and Hong Kong. In 2022, a large-scale contract reform modified both the stringency of quality targets and the number of route bundles, affecting over 40 percent of the network and providing a unique setting to study how contract design can address market power and network effects.

3.1 Tendering

Unlike fixed-price or cost-plus contracts, DTPM allocates bus service contracts through a competitive scoring auction that creates ex-ante competition among private operators. Firms submit bids for contracts that specify bundles of bus routes, each linked to a designated set of bus depots controlled by DTPM (see Figure 1). Depot proximity facilitates efficient operations, while capacity constraints limit the feasible combinations of routes that can be assigned to a given location (see Appendix Figure C.2).

Each bid includes two key decision variables: the per-kilometer price the firm is willing to accept and the fleet size it proposes to operate the bundle. These economic components are scored alongside technical criteria—such as the firm's experience in urban transit, proposed fleet characteristics, and compliance with formal requirements—using a transparent scoring rule in which the economic score receives 80–90% of the total weight. At the time of bidding, firms observe historical ridership, the depot assignment for each bundle, the regulator-set per-passenger price, and the penalty structure that governs

[1] Transfers between buses are free, and transfers between buses and the metro involve a small additional fee.

quality targets monitoring. These auction-stage choices shape both the firm's expected profits and its operational incentives under the contract. In my structural model, I treat the price and fleet size as the firm's decision variables at the tendering stage.

3.2 Operations

Beyond the tendering stage, Transantiago's contract structure creates ongoing incentives for firms to determine how to operate their assigned routes. Firms earn revenue from two components: (i) a per-passenger price set by DTPM, multiplied by the number of travelers they serve, and (ii) a per-kilometer price they bid at the tendering stage, multiplied by the kilometers they actually operate. To obtain the latter, firms must deploy transit vehicles to cover the required service, making service frequency a choice variable. Firms also choose how evenly to space departures, which determines the regularity of headways experienced by travelers. Figure 2 provides a visual representation of these two choice variables. Both frequency and headway regularity affect traveler wait times and are central to the system's service quality.

DTPM monitors these service attributes using GPS data transmitted from each bus every 30 seconds. From these data, DTPM reconstructs the realized frequency and realized headway regularity on each route. For each route, DTPM establishes quality targets for these two attributes and evaluates compliance within predefined monitoring periods whose lengths vary by time of day (typically ranging from one to three hours).

Firms incur monetary penalties whenever realized frequency or regularity falls short of the contracted quality targets in a given monitoring period. These penalties are computed using formulas written into the contracts and directly reduce firms' monthly revenues.[2] Consequently, the tendering outcomes (per-kilometer bids and fleet size) interact with operators' day-to-day choices during the contract. In my structural model in Section 6, I treat frequency and regularity as firm-specific choice variables shaped by these contractual instruments.

4 Data

My empirical analysis combines several administrative and survey datasets to study how transit contract design affects service provision and travel decisions. This section describes each dataset and how I use it in the analysis.

[2]For example, suppose a route has a contractual target of dispatching 15 buses during the morning peak (3 hours), but the operator dispatches only 13. This shortfall of two buses counts as a deviation from the frequency target for that route–period. DTPM records these deviations across periods and routes, aggregates them over time, and deducts the resulting penalties directly from the operator's monthly payment.

4.1 Mode and Route Choices

I combine individual travel choices from the 2012–2013 Household Travel Survey with reconstructed trip attributes based on operational data from the same period. The survey records all daily trips made by approximately 60,000 individuals across 18,000 randomly sampled households in the Santiago metropolitan area. The sample is representative at a fine geographic level across 866 origin–destination zones averaging 1 km^2 in size. I restrict attention to the 700 urban zones and apply sample restrictions detailed in Appendix Appendix A, yielding a final estimation sample of 47,622 trips that covers 80% of work-related trips and 83% of the city's residential population.

For each trip, I observe origin and destination coordinates, traveler demographics (income, car ownership, age, gender, education), and the chosen mode (car, public transit, walking, or other).

For car trips, I compute monetary costs using fuel prices and maintenance costs from the *Comisión Nacional de Energía de Chile*, assuming an average fuel economy of 8.3 km/liter.[3] Travel times and distances come from the OSRM routing engine, which I run on OpenStreetMap data using the exact origin–destination coordinates reported in the survey.

For public transit trips, the survey identifies the exact bus and metro routes used in each leg but does not report leg-level attributes such as fares, travel times, distances, or frequencies. To recover these, I use DTPM's trip reconstruction algorithm developed by Munizaga and Palma (2012), which combines GPS and smart-card data to infer complete itineraries, travel times, and service attributes.[4] Using this algorithm, I merge observed survey trips with corresponding route-level travel time, distance, and frequency for representative weeks in 2012 and 2013. I obtain fares separately from administrative fare tables published by DTPM. In total, I successfully match 23,400 of the 27,000 public transit trips in the survey to operational data.

Summary Statistics Appendix Tables C.1 and C.2 summarize key features of households, travelers, trip characteristics, and transit choice sets. For estimation, I restrict attention to trips made by car, public transit, or walking and bicycling, which together account for more than 95% of all trips in the survey. Most households fall into low- to middle-income brackets, and fewer than half own a private vehicle, consistent with the balanced modal split observed in the data: approximately 39% of trips are by car, 37% by public

[3] Fuel economy source: https://energia.gob.cl/sites/default/files/documentos/20240304_informe_final_estandar_-_vehiculos_medianos_vf.pdf

[4] The algorithm matches tap-in times with GPS vehicle locations to infer origins, routes, travel times, and headways. Destinations are imputed based on weekly travel patterns, and the method covers approximately 25 million trips per week.

transit, and 25% by walking. Trip distances exhibit a bimodal pattern, with short (0–2 km) and long (>5 km) trips together accounting for more than 75% of all trips. Appendix Figure C.3 shows that walking dominates short-distance travel, while car use rises sharply with income even though average travel times remain similar across groups.

Transit choice sets display substantial heterogeneity across origin–destination pairs. Direct services feature shorter travel and wait times, whereas transfer-based itineraries are more numerous, more variable, and more likely to involve the subway. During peak hours, travel times lengthen for both direct and transfer options, while wait times fall modestly due to higher scheduled frequencies. These patterns align with Appendix Figure C.4, which documents the trade-off between faster in-vehicle speeds and longer expected wait times, especially for itineraries requiring a transfer.

Together, the tables and figure highlight the rich heterogeneity in mode availability, service quality, and route complexity that underlies travelers' mode and route choices in Santiago.

4.2 Frequency and Headway Regularity Choices

I use GPS data from DTPM covering the entire Transantiago bus network between August 2022 and August 2023. Each vehicle transmits its location every 30 seconds, and the dataset records the route, operator, vehicle ID, timestamp, and coordinates. These data are used by DTPM to monitor quality targets and enforce penalties, and they achieve full coverage across firms, routes, and days with no systematic gaps during the observation window.

I construct the two service attributes that constitute the firm-controlled dimension of service quality, which given their central role in operational decisions I treat as the primary choice variables in the structural model in Section 6.

The first attribute is frequency, which measures how many buses a firm dispatches on a route during a time interval. For comparability across routes and monitoring periods, I report frequency in buses per hour. The second attribute is regularity, which captures how consistent the intervals between consecutive buses are. I measure regularity using the coefficient of variation of headways computed within each monitoring period. The coefficient of variation equals the standard deviation of headways divided by their mean, so it scales headway dispersion relative to the typical spacing of buses. This makes the regularity measure comparable across routes that operate at different frequencies. A value of zero indicates perfectly regular service, while larger values represent increasingly irregular and unreliable service.

Figure 2 provides a visual introduction to these service attributes. Each line corresponds to one bus dispatch and shows the distance traveled over time. The number of lines between 6am and 7am reflects frequency in that hour, while the variability in spacing

between lines reflects regularity. The trajectories also reveal two operational patterns. First, even at the start of the route, dispatches are not perfectly evenly spaced, which creates initial variation in headways. Second, this variation amplifies as buses progress along the corridor, generating the familiar bus bunching pattern in which small spacing differences accumulate into clusters of buses followed by long gaps with no service.

For the empirical analysis, I aggregate these measures to the route-day level, excluding night service (12am–5am) and dispatches flagged by DTPM as exempt from performance evaluation, yielding a panel of 549,000 route-day observations. In addition to frequency and regularity, the GPS data provide route-level characteristics that shape operational costs and performance, including route length, average operating speed, and the bundle to which each route is assigned. Linking routes to bundles also allows me to construct bundle-level aggregates such as the number of depots and routes associated with each contract. These features complement the choice variables and help characterize the supply environment in which firms operate.

Summary Statistics Appendix Table C.3 summarizes system, bundle, and route level characteristics using route-day observations from August 2022 and August 2023, which represent the system's initial and final equilibrium states.

At the system level, the network comprises roughly 350 routes operated from more than 60 depots. Bundles differ substantially in size and complexity: the number of routes spans from 11 to 89 and the number of depots ranges from 2 to 19. At the route level, frequency averages 5.8 buses per hour but ranges from 1 to more than 20, while headway regularity exhibits meaningful dispersion with coefficients of variation between 0.02 (near-perfect regularity) and 1.42. Routes are on average 18.5 km long but range from short feeders of 2–3 km to long trunks exceeding 50 km. Operating speeds average 17.8 km/h, with congested corridors falling below 5 km/h and faster segments reaching nearly 40 km/h. This rich variation in length, speed, and service attributes highlights the diverse operating conditions faced by firms and the differences in route-level cost environments.

Appendix Figure C.5 plots the joint distribution of frequency and regularity across route-days and highlights the operational trade-offs that motivate the structural model. Even at relatively low frequencies, many route-days exhibit sizable irregularity, with coefficients of variation around 0.5. The upward-sloping pattern indicates that higher-frequency routes tend to experience greater irregularity, reflecting the difficulty of maintaining consistent headways as dispatch rates increase. Because frequency and regularity directly determine traveler wait times and ultimately service quality, DTPM enforces compliance through quality targets specified in the contract.

4.3 Equilibrium Outcomes: Travel Time, Traffic Flow, and Ridership

First, I measure public transit ridership using smart-card transaction data that record all system tap-ins. These data provide route-level boardings in 30-minute intervals for every day in the observation period, covering approximately 3.5 million trips per weekday. I use these data to examine whether more stringent quality targets increase ridership at the route level in Section 5.

Second, I use vehicle count data from 64 automatic traffic sensors distributed across major corridors in Santiago. These sensors record vehicle flows in 15-minute intervals. I complement these data with travel speed measures from the Google Maps API, matched to the same locations and timestamps. The traffic flow and speed data span the period from August 1 to September 17, 2022, and were originally collected by Bordeu (2023) in collaboration with the Chilean Ministry of Transportation.

Summary Statistics Appendix Table C.3 reports descriptive statistics for transit ridership at the system, bundle, and route levels. At the system level, daily ridership averages roughly 1.9 million passengers, reflecting the scale of Santiago's public transit network. Bundle-level ridership varies widely, ranging from about 50,000 to more than 550,000 passengers per day, consistent with large differences in bundle size, especially after the contract reform. Appendix Figure C.6 shows the evolution of these patterns over time: ridership is unevenly distributed across operators, with a small number of firms accounting for a large share of total boardings while others operate bundles with substantially lower demand.

Appendix Figure C.7 summarizes the traffic flow and speed data. Panel (a) maps the locations of the 64 automatic traffic sensors across major corridors in Santiago, illustrating broad coverage of the primary arterials used by both cars and buses. Panel (b) plots the empirical flow–travel time relationship at these locations, revealing the congestion pattern that underlies the road technology: travel times increase sharply once traffic flows on a corridor approach its capacity.

I use this combination of traffic flow and speed data to estimate a road technology that maps vehicle flows to travel times. This relationship allows me to predict how equilibrium travel speeds adjust when transit service quality or car usage changes endogenously in the model.

5 Descriptive Evidence

In late 2022, DTPM implemented a major contract reform as part of its regular renewal cycle, which affected more than 40 percent of routes.[5] The reform changed two elements of contract design. First, quality targets became stricter, as DTPM monitored compliance with these targets more frequently, increasing the effort transit operators needed to exert to avoid penalties.[6] Second, DTPM rebundled routes into a larger number of smaller packages, altering the share of the network controlled by each transit operator and increasing network fragmentation across transit operators. Because each treated route entered the renewal process solely based on its preset contract expiration date, exposure to these changes is orthogonal to contemporaneous service attributes.

These contract modifications affected firms asymmetrically: some operators lost most of their routes, others retained a subset, and at least one preserved their full network. This heterogeneity generates distinct sources of variation that can be used to examine the effects of contract design on service outcomes. In this section, I present descriptive evidence along two margins. First, I study how stricter quality targets affected firms' provision of frequency and headway regularity, as well as the induced ridership response. Second, I analyze how network fragmentation—shaped by bundle size and operator assignment—affects market power and coordination across routes within origin–destination trips. These reduced-form results provide evidence on the mechanisms through which contract design influences service quality and welfare, and they motivate the structural analysis that follows.

5.1 Effect of Quality Targets on Service Attributes

Figure 3 illustrates deviations from planned service attributes in the pre-reform period (August to December 2022). Firms closely adhered to frequency targets, with bunching around zero deviation, but systematically deviated from headway regularity targets by providing more irregular dispatches. This pattern suggests that the monetary penalties for non-compliance were less costly than achieving stricter regularity, leading firms to tolerate penalties rather than invest in coordination. To test whether tighter quality targets can shift this trade-off, I exploit the introduction of more stringent monitoring rules during contract retendering.

[5] Transit contracts in Transantiago are medium-term, typically lasting 5–7 years.

[6] DTPM standardized monitoring from irregular 2–3 hour intervals to uniform 30-minute windows.

Empirical Strategy To measure the effect of stricter quality targets on service attribute outcomes, I estimate the following specification:

$$\log(y_{rdkt}) = \sum_{l \neq -1} \beta_l \, \text{Treated}_r \cdot \mathbb{1}\{t = l + 1\} + \mu_r + \lambda_k + \delta_t + X'_{rt}\phi + \varepsilon_{rdkt}, \tag{4}$$

where y_{rdkt} denotes service outcomes for route r operated by firm k from depot d on day t. I focus on frequency, headway regularity (coefficient of variation), and passenger ridership. Treated_r is an indicator for routes subject to stricter quality targets. The specification includes route fixed effects (μ_r), firm fixed effects (λ_k), and date fixed effects (δ_t). X_{rt} controls for time-varying route characteristics such as distance and planned service attributes. Standard errors are clustered at the firm level. The sample spans August 2022 to August 2023.

Because treated routes entered the renewal process based on preset contract expiration dates, exposure to stricter quality targets is orthogonal to contemporaneous service attributes. The control group consists of routes operated by the only firm that was entirely unaffected by the contract reform, meaning its quality targets and route bundle composition remained unchanged. A causal interpretation of the event-study coefficients requires that, absent the reform, treated and control routes would have followed parallel trends and that control routes are not affected by the treatment of other routes. However, the network structure raises the possibility that travelers substitute between nearby routes, which could induce spillovers and violate SUTVA. To mitigate this concern, I restrict the control group to routes serving geographically distinct origin–destination (O–D) pairs from treated routes, limiting the scope for substitution-driven changes in control outcomes. Appendix Figure C.8 shows that overlap across O–D choice sets is minimal. I compare treated and untreated routes before and after their respective renewal dates. The staggered rollout of the reform provides differential timing in treatment and allows the event-study coefficients β_l to summarize how service outcomes evolve around the implementation of stricter quality targets.

Results Figure 4 and Figure 5 report the event-study estimates. Treated and control routes exhibit parallel pre-trends, providing suggestive support for the identification assumption. The dynamic coefficients show that the reform generated heterogeneous responses across service attributes, consistent with pre-reform compliance patterns. To complement the event-study evidence, Table 2 reports the corresponding average post-treatment effects from the static difference-in-differences specification. The two sets of results align closely.

For frequency, stricter quality targets lead to a modest and statistically insignificant increase of about 2.7 percent, reflecting that operators were already meeting frequency requirements. In contrast, regularity responds strongly: the coefficient of variation

of headways declines by roughly 16 percent, indicating a substantial improvement in dispatching consistency. Finally, ridership increases by about 11 percent on treated routes relative to controls. The effects on regularity and ridership are statistically significant at the 5 percent level in both the dynamic and static estimates, emerge immediately after implementation, and remain stable throughout the post-reform period.

Discussion The results point to a two-step adjustment pattern. Firms respond to stricter monitoring by improving the attribute where deviations were most frequent: headway regularity. The sharp decline in headway variation indicates that operators had the capacity to provide more regular service but lacked incentives to do so under weaker enforcement. Passengers then respond to the improvement in regularity, as reflected in higher ridership. The contrast between modest frequency changes and large gains in regularity highlights a key margin in service provision. Increasing frequency is less coordination-intensive, while improving regularity requires greater dispatching effort, monitoring, and operational oversight. That firms adjust along this more demanding margin under stricter targets suggests that coordination yields meaningful benefits. Quantifying these trade-offs calls for the structural framework developed below, which evaluates how alternative contract designs balance the welfare gains from stricter quality targets against the costs of providing more regular service.

5.2 Effect of Network Fragmentation on Service Attributes

Figure 6 provides a visual example of network fragmentation. When routes that previously belonged to the same operator are reassigned to different operators, the network becomes fragmented. This fragmentation can limit the ability of operators to coordinate headways across routes, potentially worsening regularity and increasing traveler waiting times. To formally test this hypothesis, I relate variation in market concentration, measured by the Herfindahl–Hirschman Index (HHI), to observed service attributes in the pre-reform period.

Empirical Strategy To measure the correlation between network fragmentation and service attributes, I estimate the following specification:

$$\log(y_{itod}) = \beta \log(\text{HHI}_{itod}) + \alpha_i + \alpha_t + \alpha_{od} + X'_{itod}\gamma + \varepsilon_{itod}, \tag{5}$$

where y_{itod} denotes one of three outcomes for trip i between origin o and destination d on date t: aggregate frequency, the aggregate coefficient of variation of headways, or expected wait time. HHI_{itod} measures network concentration at the trip–OD–date level. The

specification includes trip fixed effects (αi), date fixed effects (α_t), and origin–destination fixed effects (α_{od}). X_{itod} controls for planned frequency and the number of routes in the choice set. Standard errors are clustered at the traveler level.

I restrict attention to the pre-reform period (August to December 2022) to avoid confounding effects from the change in quality targets implemented at the end of 2022 (see Figures 6c and 6d). For each trip in the household travel survey and each day in this period, I construct a trip-specific route choice set containing all feasible routes and their observed attributes. I compute route-level market shares using planned frequency (which is predetermined by contract and not a firm decision) and use these shares to construct the Herfindahl–Hirschman Index for each trip–OD–date.

Because operators served different route bundles and the composition of these bundles changed during the period of analysis, the effect of network fragmentation is identified from variation across days within a market.

Results Table 1 presents the regression estimates. The coefficient of interest, β, is the elasticity of service outcomes with respect to market concentration. In column (1), a 10% increase in HHI is associated with a 1.59% reduction in aggregate frequency. In column (2), the same 10% increase in HHI is associated with a 2.44% reduction in the coefficient of variation of headways, indicating improved regularity. Finally, in column (3), a 10% increase in HHI reduces expected waiting time by 0.23%. Taken together, these results imply that higher market concentration decreases service frequency but improves headway coordination, with the latter effect dominating to slightly reduce expected wait times on net. All effects are statistically significant at the 1% level.

Discussion The results highlight two distinct channels through which network fragmentation affects service quality. On the one hand, higher concentration reduces aggregate service frequency. This suggests that dominant firms may exercise market power by reducing costly service provision. On the other hand, an increase in concentration lowers the coefficient of variation of headways. This pattern is consistent with the idea that fragmented markets suffer from poorer coordination across operators, while concentrated markets can better schedule departures to avoid bus bunching. Finally, the wait time reductions suggest that the coordination effect slightly dominates the frequency effect in terms of passenger outcomes. In other words, the efficiency gains from more regular headways are just strong enough to offset the loss of frequency. This provides suggestive evidence that in this setting, coordination externalities are quantitatively important and can partially mitigate the service quality losses associated with market power. These findings motivate the counterfactual analysis using a structural model, where I examine how alternative contractual instruments—such as bundling routes under common operators

or enforcing stricter quality targets—can influence the balance between market power and network effects.

6 Empirical Model

The descriptive evidence in Section 5 suggests that quality targets and route bundling meaningfully shape service provision and traveler responses. It also reveals trade-offs that reduced-form analysis cannot fully quantify. In particular, how stricter quality targets and rebundling affect operator costs and revenues, how these policy tools interact in equilibrium, and how alternative designs shape welfare.

To address these questions, I turn to an empirical model. The model features three agents: travelers choosing transportation modes and public transit routes; private transit operators choosing service attributes; and a transit agency setting fares for travelers and contract terms for operators.

The model characterizes the interaction between travel demand and transit service provision in a regulated oligopolistic environment. Travelers' mode and route choices determine ridership patterns and road congestion, which affect operators' revenues, operating costs, and thus service attribute choices. Transit operators' service attribute choices—particularly frequency and headway regularity—determine wait times, which affect traveler choices. I estimate the preference and cost parameters that govern these choices. Using these primitives, I solve for the equilibrium under counterfactual contract designs and provide direct comparative statics of service quality, ridership, traffic congestion, and social welfare.

The model assumes that travelers' origins and destinations are determined ex ante and examines mode and route choices given these fixed trip patterns. This assumption is motivated by three considerations. First, for most urban trips, origins and destinations reflect longer-term residential and employment decisions that respond slowly to transportation policy changes. Second, the contract parameter variation I exploit occurred over a relatively short time horizon, making it unlikely that fundamental location patterns adjusted significantly. Third, incorporating joint location-transportation choices would substantially complicate the empirical analysis given the rich individual-level preference heterogeneity I incorporate into the model.

This model offers two methodological advantages. First, I estimate cost parameters from rich operational data on service choices, leveraging quasi-experimental policy variation for identification. This avoids reliance on prices or auction bids, which are scarce in regulated settings with medium-term contracts: auctions are infrequent and post-award prices do not vary. Second, I estimate preference parameters using both mode and route

choices. This allows me to capture substitution and complementarities across routes, which is essential for understanding how bundling routes under an operator affects network performance. The model also treats wait time explicitly, the margin most directly shaped by operators' choices and one that the empirical literature has estimated to exceed the value of in-vehicle travel time.

To guide interpretation, I outline the modeling choices that shape the scope of the analysis. I focus on a static equilibrium, which is appropriate for studying how contract design affects service provision and traveler choices in steady state. I take origins, destinations, and the route network as given, since the goal is to evaluate how existing routes should be allocated across operators and how their performance should be monitored, rather than to redesign the network. I model road congestion affecting car travel times, but I abstract from crowding on transit vehicles, which is more relevant for peak-load or capacity-planning questions than for contract incentives. Finally, I concentrate on the three dominant travel modes (car, public transit, walking), abstracting from smaller-share options such as taxis and ride-sharing.

6.1 Travelers

Travelers make decisions in two sequential stages: first choosing among transportation modes, then, conditional on selecting public transit, choosing among available routes. This two-stage structure captures not only substitution among transportation modes but also substitution among transit routes in response to endogenous service attributes that reflect transit operators' responses to contract design.

6.1.1 Stage 1: Mode Choice

For a given origin-destination pair (market m), traveler i's utility from choosing mode j is given by:

$$u_{ijm} = \theta_{ij} + v_{jm} + \boldsymbol{\chi}_{jm} + \epsilon_{ijm} \tag{6}$$

where θ_{ij} is a mode-specific random coefficient that varies across individuals, v_{jm} is the deterministic utility component, $\boldsymbol{\chi}_{jm}$ represents observable mode-market characteristics, and ϵ_{ijm} is an idiosyncratic error term assumed to follow a Type I extreme value distribution.

The choice set includes three transportation modes: car, public transit, and walking (the outside option). Mode availability depends on individual circumstances and infrastructure access. For car availability, the Household Travel Survey data indicates whether individuals have access to a vehicle. For transit accessibility, I identify all bus stops and subway stations

within 1,000 meters of both trip origins and destinations, determining the set of transit routes serving these access points.

The deterministic utility component v_{jm} varies by transportation mode:

$$v_{jm} = \begin{cases} \mathbb{E} \max_{r \in \mathcal{R}_m} u_{rm}, & \text{if } j = \text{transit} \\ \alpha_{\text{price}} P_{jm} + \alpha_{\text{veh}} T_{jm}^{\text{veh}}, & \text{if } j = \text{car} \end{cases}$$

For car travel, the deterministic utility depends on trip cost P_{jm} and travel time T_{jm}^{veh}. Trip costs include both fuel expenses and maintenance costs.[7] For public transit, the deterministic utility equals the expected maximum utility across all available routes $\mathcal{R}_m$ in market m, which I discuss in Section 6.1.2, where I provide details of the route choice model. Walking serves as the outside option with utility normalized to zero, ensuring model identification and providing a baseline for comparing other transportation modes.

The observable characteristics χ_{jm} include three sets of fixed effects interacted with mode indicators. First, I include mode-specific fixed effects to capture average preferences across transportation options. Second, I incorporate mode-trip characteristic interactions, where trip variables include distance, purpose, time period, and indicators for whether trips originate or terminate in the central business district. Third, I include mode-demographic interactions with traveler characteristics including education, age, and gender.

Individual heterogeneity enters through the mode-specific random coefficient θ_{ij}, which allows baseline preferences for each transportation mode to vary across travelers. This specification maintains tractability while capturing unobserved preference heterogeneity that affects mode choice decisions.

Choice Probabilities Given the Type I extreme value distribution assumption for ϵ_{ijm}, the probability that traveler i chooses mode j in market m follows a standard logit specification:

$$\mathbb{P}_{ijm} = \frac{\exp(\theta_{ij} + v_{jm} + \chi_{jm})}{\sum_{k \in J_m} \exp(\theta_{ik} + v_{km} + \chi_{km})}$$

where J_m represents the set of available modes in market m.

6.1.2 Stage 2: Transit Route Choice

The traveler chooses among transit route options $h \in \mathcal{H}_m$ in market m (origin-destination pair). Building on the model developed by Kreindler *et al.* (2023), each option h consists

[7] Fuel expenses are calculated as the product of distance, fuel efficiency, and gasoline prices. Maintenance costs are calculated as the product of distance and by per-kilometer maintenance rates

of either a direct route r or a combination of two routes r_1 and r_2 connected through a transfer. The utility from option h depends on a deterministic component and a random wait time component:

$$u_h = v_h + \alpha_{\text{wait}} T_h^{\text{wait}} \tag{7}$$

This model assumes that bus arrivals on route r follow a Poisson process with arrival rate λ_r. This generates exponentially distributed wait times with the property that $\Pr(T_r^{\text{wait}} > w) = \exp(-\lambda_r w)$. Figure C.9 shows that this distributional assumption is broadly consistent with the empirical distribution of traveler wait times computed from GPS-based headway data. The exponential benchmark provides a close approximation, particularly for routes with higher arrival rates.[8]

The deterministic utility component v_h is given by:

$$v_h = \begin{cases} \alpha_{\text{price}} P_h + \alpha_{\text{veh}} T_h^{\text{veh}}, & \text{if } h = \text{Direct} \\ \alpha_{\text{price}} P_h + \alpha_{\text{veh}} T_{r_1}^{\text{veh}} & \\ \quad + \mathbb{E} \max_{r_2} \left[\alpha_{\text{veh}} T_{r_2}^{\text{veh}} + \alpha_{\text{wait}} T_{r_2}^{\text{wait}} \right] + \mu_{\text{transfer}}, & \text{if } h = \text{Transfer} \end{cases}$$

P_h is the fare for option h, T_h^{veh} is in-vehicle travel time, T_h^{wait} is wait time governed by the Poisson arrival process, and μ_{transfer} captures the pure disutility of making a transfer.

For direct routes, utility depends on the price, in-vehicle time, and realized wait time for that route. For transfer options, the traveler experiences utility from the first leg (including its wait time) plus the expected utility from optimally choosing among available second-leg routes at the transfer station. This expected utility formulation captures the option value from having multiple connections available at transfer points.

Transit Choice Set I determine route choice sets using detailed origin-destination information from the Household Travel Survey combined with complete network topology data. The choice set $\mathcal{H}_m$ for market m includes all direct routes and single-transfer combinations that connect the accessible origin and destination stations. Choice set sizes vary substantially across markets, with a median of 8 options, ranging from a minimum of 1 to a maximum of 32 available combinations.

Choice Probabilities The exponential wait time assumption yields tractable expressions for choice probabilities and expected utility. The probability of choosing option h among

[8] As shown in Figure C.9, the exponential distribution fits the observed wait time distribution more closely for routes with higher service frequencies (larger λ_r), where random arrival patterns are more likely to emerge.

alternatives ranked by deterministic utility $v_1 \leq v_2 \leq \cdots \leq v_H$ is:

$$\lambda_h^{-1}\pi_h = \sum_{i=1}^{h} e^{-\alpha_{\text{wait}}^{-1} M_i} \frac{e^{v_i \alpha_{\text{wait}}^{-1} \Lambda_i} - e^{v_{i-1} \alpha_{\text{wait}}^{-1} \Lambda_i}}{\Lambda_i}$$

where $\Lambda_i = \sum_{j=i}^{H} \lambda_j$ and $M_i = \sum_{j=i}^{H} v_j \lambda_j$, with $v_0 = -\infty$ by convention.

This framework ensures computational tractability and avoids the Independence of Irrelevant Alternatives (IIA) property problem that affects standard logit models, as combining identical routes with split frequencies yields identical choice probabilities and expected utilities.

Expected Utility The expected utility from choosing optimally among available routes is:

$$\mathbb{E} \max_{h \in \mathcal{H}_m} u_h = v_{h^*} - \pi_{h^*} \frac{\alpha_{\text{wait}}}{\lambda_{h^*}}$$

where h^* denotes the option with highest deterministic utility v_{h^*}, π_{h^*} is the probability of choosing option h^*, and λ_{h^*} is its effective frequency (arrival rate). The influence of alternative options $h \neq h^*$ on expected utility is captured through the choice probability π_{h^*}. That is, when more attractive alternatives are available, the probability of choosing any single option decreases, increasing the expected utility from the entire choice set.

Linking Supply Decisions to Arrival Rates The main departure from Kreindler *et al.* (2023) is connecting service attribute decisions to the effective frequency λ_r that determines traveler wait times. Transit operators choose both frequency and headway regularity (measured by the coefficient of variation of headways) for each route r in their bundle.

I model the relationship between these service attribute decisions and travelers' experienced effective arrival rates using the following engineering relationship:

$$\lambda_r = \frac{f_r}{1 + \text{CV}_r^2}$$

where f_r is the number of dispatched buses per interval of time and CV_r is the coefficient of variation of headways. When service is perfectly regular ($CV_r = 0$), travelers experience the full dispatched frequency. As service becomes more irregular, the effective frequency decreases, reflecting longer average wait times due to service bunching and gaps.

This specification captures an important operational trade-off: operators can increase service quality either by running more buses (higher frequency) or by improving service reliability (lower coefficient of variation). The contractual instruments I examine—quality targets and route bundling—affect operators' incentives along both dimensions.

6.2 Private Transit Operators

Private transit operators make decisions in two sequential stages: first bidding competitively for bundles of routes in government tenders, then choosing service attributes (frequency and headway regularity) for each route in their awarded bundle. This two-stage structure captures the key trade-offs operators face between service quality and costs, and between regulatory compliance and profit maximization. Crucially, operators make bundle-level decisions that account for both shared depot resources and demand spillovers across routes, enabling them to internalize network effects within their bundle while potentially fragmenting coordination across bundles operated by different firms.

6.2.1 Stage 2: Operations

Each firm k at time t operates a set of routes $\mathcal{R}_k$. Each route $r \in \mathcal{R}_k$ is assigned to a depot $d(r)$, which affects its operating costs. The firm's operational profit is:

$$\Pi_{kt}^{\text{op}} = \sum_{r \in \mathcal{R}_k} \Big(\text{Revenue}_{rt} - \text{Penalties}_{rt} - \text{Operational Costs}_{rt} \Big), \tag{8}$$

where $\text{Operational Costs}_{rt}$ implicitly depend on $d(r)$. To keep notation concise, I omit the depot index and maintain the route-time subscript rt throughout the analysis. This structure captures the central trade-offs between service quality, regulatory compliance, and cost minimization. I now detail each component of the profit function.

Revenue Firm revenue comes from two sources, a demand-based and a distance-based component. The demand-based component captures passenger revenue:

$$R_{kt}^{\text{pax}} = p_k^{\text{pax}} \sum_{r \in \mathcal{R}_k} q_{rt}$$

where ridership q_{rt} depends on both the service attributes of route r and the service attributes of other routes, capturing demand spillovers within and across route bundles. The per-passenger price p_k^{pax} is set by the transit agency.

The distance-based component captures revenue for kilometers of service supplied:

$$R_{kt}^{\text{dist}} = p_k^{\text{dist}} \sum_{r \in \mathcal{R}_k} f_{rt} L_r^s$$

where L_r^s is the route service distance. The per-kilometer price p_k^{dist} is determined in the competitive tender and fixed in the contract. Unlike passenger revenue, this component is purely mechanical: it scales linearly with service kilometers.

This dual revenue structure creates incentives for both ridership maximization and service provision.

Penalties and Quality Targets The transit agency establishes explicit quality targets for frequency $\bar{f}_r$ and implicit quality targets for service regularity $\bar{CV}_r$ for each route, with penalties for deviations:

$$\mathcal{P}^f_{rt}(f_{rt}, \bar{f}_r) = \max\{0; \tau^f \cdot (\bar{f}_r - f_{rt})\}$$
$$\mathcal{P}^{\text{wait}}_{rt}(f_{rt}, \bar{f}_r, CV_{rt}, \bar{CV}_r) = \max\{0; \tau^w \cdot (W_{rt} - \bar{W}_r)\}$$

where W_{rt} is the realized average wait time and $\bar{W}_r$ is the target wait time. The relationship between service attribute choices and expected wait time follows the engineering formula:

$$W_{rt} = \frac{1}{2f_{rt}} \cdot (1 + CV^2_{rt})$$

This specification captures how both frequency and headway regularity affect passenger wait times, providing the link between supply-side operational decisions and demand-side service quality. While $\mathcal{P}^f_{rt}$ penalizes undersupply of frequency directly, $\mathcal{P}^{\text{wait}}_{rt}$ internalizes the combined effect of frequency and regularity on waiting times.

Operational Costs Transit operations are labor intensive. The cost structure should link labor inputs to the service attributes chosen by firms. The starting point is the vehicle-hour requirement implied by a given frequency and route characteristics:

$$\text{Vehicle-hours}_{rt} = f_{rt} \cdot \frac{L^T_r}{s_{rt}},$$

where L^T_r denotes the route distance including deadhead travel from the depot to the route origin, and s_{rt} is the average route speed. L^T_r differs from the service distance L^s_r that generates distance-based revenue, emphasizing the role of depot location in shaping costs.

Labor demand depends on both the scale and the quality of service provision. While vehicle-hours capture the quantity dimension, regularity requires additional managerial inputs such as dispatching and monitoring. I represent the production technology for composite labor demand as:

$$\text{Labor}_{rt} = \left(f_{rt} \cdot \frac{L^T_r}{s_{rt}}\right)^{\gamma} \cdot g(CV_{rt}),$$

where γ is an elasticity mapping vehicle-hours into labor units, and $g(CV_{rt})$ captures

the incremental labor effort required to improve headway regularity. I parameterize $g(CV_{rt}) = CV_{rt}^{-\phi}$ with $\phi > 0$, so that reducing the coefficient of variation of headways entails increasing marginal labor demand.

Route-level costs follow directly from multiplying labor demand by the input price. In addition, I allow for depot-level scale effects. Routes sharing a depot benefit from common resources such as maintenance facilities, supervisory staff, and spare vehicles. Rather than modeling depot aggregation explicitly, I incorporate these effects directly into the route-level specification. Combining the three dimensions quantity, quality, and scale effects yields:

$$C_{rt} = w_k \cdot \left(f_{rt} \cdot \frac{L_r^T}{s_{rt}} \right)^{\gamma} \cdot CV_{rt}^{-\phi} \cdot |\mathcal{R}_{dkt}|^{\rho} \cdot \varepsilon_{rt}, \tag{9}$$

where w_k is the firm-specific wage rate, $|\mathcal{R}_{dkt}|$ is the number of routes operated from depot d, and ε_{rt} captures route-level productivity shocks. A negative ρ reflects economies of scale, while a positive ρ reflects congestion effects. This expression captures the three key dimensions of operational costs: service quantity, service quality, and scale effects.

Optimality Conditions Transit operators maximize operational profit Π_k^{op} by choosing frequency f_{rt} and regularity measured by the coefficient of variation of headways CV_{rt}.

The first-order conditions for optimal frequency and regularity are:

$$\frac{\partial C_{rt}}{\partial f_{rt}} = p_k^{\text{pax}} \left[\frac{\partial q_{rt}}{\partial f_{rt}} + \sum_{u \neq r} \frac{\partial q_{ut}}{\partial f_{rt}} \right] + p_k^{\text{dist}} L_r^s - \frac{\partial \mathcal{P}_{rt}^f}{\partial f_{rt}} - \frac{\partial \mathcal{P}_{rt}^{\text{wait}}}{\partial f_{rt}}$$

$$\frac{\partial C_{rt}}{\partial CV_{rt}} = p_k^{\text{pax}} \left[\frac{\partial q_{rt}}{\partial CV_{rt}} + \sum_{u \neq r} \frac{\partial q_{ut}}{\partial CV_{rt}} \right] - \frac{\partial \mathcal{P}_{rt}^{\text{wait}}}{\partial CV_{rt}}$$

These conditions show that optimal service attribute decisions balance marginal costs against four sources of marginal benefit: direct ridership effects on the route, demand spillovers to other, distance-based revenue, and the avoidance of regulatory penalties. The presence of demand spillovers $\sum_{u \neq r} \frac{\partial q_{ut}}{\partial f_{rt}}$ illustrates how firms internalize cross-route demand interactions within their bundle, a key mechanism for evaluating the welfare effects of bundling.

6.3 Road Technology

I model the road network as a directed graph, similar to Almagro *et al.* (2022). Each node represents a bus stop l and edges connect contiguous bus stops (see Figure C.10). I assume that car routes are exogenous and travelers take the route suggested by Google Maps. The

transit network is fixed but travelers choose which route or combination of routes to take, as explained in Section 6.1.2. A traveler going from bus stop l to bus stop l' follows a directed path over edges that connects l and l'.

During period n, the total vehicle flow on edge e is:

$$V_{en} = \sum_j \omega_j V_{enj}, \tag{10}$$

where V_{enj} is the total number of vehicles of mode j going through e and weights ω_j capture the fact that cars and buses may have different effects on congestion. For cars, the number of vehicles is a function of trips $V_{enj} = \sum_{m \in \mathcal{M}^e_{nj}} q_{mj}$, where $\mathcal{M}^e_{nj}$ is the set of all markets in which travelers take a route that goes through edge e. For buses, the number of vehicles is a function of frequencies $V_{enj} = \sum_{r \in \mathcal{R}^e_{nj}} f_{rj}$, where $\mathcal{R}^e_{nj}$ is the set of bus routes that go through e.

For road-based modes, the travel time over edge e at period n for mode j is given by:

$$T^{\text{veh}}_{enj} = \max\{T^0_{ej}, A_{enj} \cdot V^{\eta}_{en}\}. \tag{11}$$

For every pair of neighboring bus stops, there is a range with low vehicle flows for which the travel time is independent of vehicle flows. Travel time is then equal to an edge-mode specific *free-flow time* T^0_{ej} that captures road infrastructure and geography (including distance). The second term inside the maximum represents the range in which travel times increase with vehicle flows. Over that range, I assume a constant elasticity η of travel times to vehicle flows. A_{enj} is an edge-mode specific scale factor that captures geography and road infrastructure.

7 Estimation

7.1 Travel Preference Parameters

I estimate the set of travel preference parameters $\Omega = \{\theta_{ij}, \alpha_{\text{price}}, \alpha_{\text{veh}}, \alpha_{\text{wait}}, \mu_{\text{transfer}}\}$ for mode and route choice via Simulated Maximum Likelihood Estimation (MLE). I provide the estimation details in Appendix B.1.

Identification The identifying variation comes from the rich variation in choice alternative characteristics and observed choices made by travelers. The cost, in-vehicle travel time, wait time, and transfer penalty parameters are informed by how differences in these attributes across choice alternatives affect the relative odds of choosing different modes and

routes.[9] With choice sets ranging from 1 to 32 transit route options (median of 8), there is substantial cross-sectional variation in the attractiveness of transit relative to car travel and in the composition of available route alternatives.

I include an extensive set of fixed effects and control variables to address potential sources of bias in preference parameter estimation. The specification includes mode-specific fixed effects, mode-trip characteristic interactions (including trip distance, purpose, time period, and central business district (CBD) origin/destination indicators), and mode-demographic interactions with traveler characteristics including education, age, and gender. These interactions control for a rich set of time-varying and location-specific unobservables by travel mode.

Parameter Estimates Table 3 reports the travel preference parameter estimates under four specifications. Columns (1)–(3) progressively add interactions of mode dummies with trip-related and demographic characteristics, while column (4) allows for random coefficients on mode dummies. Across all specifications, the coefficients are stable in magnitude and highly significant, which suggests that the estimates are not driven by specification choice.

The estimates indicate that commuters place a substantially higher disutility on waiting relative to in-vehicle travel time. In column (4), the marginal utility of one hour of waiting time is about 8.4, compared to 4.7 for an hour of travel time. This implies that waiting is valued at roughly 1.8 times in-vehicle travel, a ratio consistent with the literature and reinforcing the role of service frequency in determining demand. The implied willingness to pay for an additional bus per hour, shown in Figure 7a, highlights the steep marginal value passengers place on frequency improvements.

Cost sensitivity is also precisely estimated, with a marginal utility of -0.42 per dollar. Combining the time and cost coefficients yields an average value of travel time (VOT) between \$10.9–\$11.4 per hour across specifications, in line with benchmarks for urban commuting contexts. The transfer penalty is around -0.98 in utility units, which translates into a time-equivalent disutility of about 12–13 minutes of in-vehicle time. This penalty reflects the inconvenience of making a connection above and beyond the mechanical time costs of transferring.

Column (4) introduces heterogeneity in preferences for modes, with statistically significant random coefficient estimates for both car and transit dummies.[10] The standard

[9] The fare structure P_{lt} varies across options within markets. While bus-to-bus transfers incur no additional cost, bus-to-subway transfers require an additional reduced fare, generating price variation that helps identify travel cost sensitivity.

[10] For the specification with random coefficients, since there is no closed form for choice probabilities when integrating out the random preference distribution, I simulate the choice probabilities using Monte Carlo integration with a sequence of 100 Halton draws. This simulation approach maintains computational tractability while allowing for unobserved preference heterogeneity that is essential for welfare analysis.

deviations are sizeable (0.63 for car, 0.85 for transit), indicating meaningful dispersion in mode-specific tastes beyond observed demographics or trip features. This heterogeneity is important when simulating counterfactuals, as it governs substitution patterns in mode choices.

Taken together, these estimates underscore two main findings. First, wait time carries a disproportionate weight in commuter utility, which strengthens the rationale for policies that target service attributes such as frequency or regularity. Second, transfer penalties are sizeable but not dominant, suggesting that improving network connectivity may generate meaningful but more modest gains relative to frequency improvements.

7.2 Cost Parameters

I estimate the set of cost parameters $\Psi = \{\gamma, \phi, \rho\}$ for service attribute choices via Generalized Method of Moments (GMM). I provide the estimation details in Appendix B.2.

Identification Estimating the parameters of the route-level cost function in equation (9) is challenging because the variables of interest are chosen by firms, raising concerns about endogeneity. I address this using two complementary sources of exogenous variation. First, the contract reform introduced stricter quality targets for some routes and rebundled these routes across depots. I exploit this variation to identify the parameters linked to regularity and depot load. Second, for frequency and route speed, I rely on exogenous shocks or features of the network design. Below, I discuss the potential sources of bias for each variable and the instruments or assumptions I use to address them.

Frequency is chosen by operators and may respond to unobserved demand shocks. I instrument frequency with exogenous operational shocks—such as vehicle breakdowns, blockages, and other unexpected incidents—that constrain the number of buses that can be dispatched but are not systematically related to passenger demand.

Headway regularity may be correlated with unobserved productivity or demand conditions, for example if firms exert greater effort on high-demand routes. To address this concern, I exploit stricter quality targets introduced only for routes under new contracts, while old contract routes retained previous standards. This regulatory variation shifts the cost of achieving regularity but does not directly affect passenger preferences, since contract terms are not observed by travelers.

Depot load can be endogenous if more routes are allocated to more efficient depots or to high-demand areas. To address this, I use depot reallocations from the reform's rebundling process, focusing on old contract routes that experienced depot changes but unchanged quality standards. These administrative reallocations altered depot load orthogonally to

route-specific demand or productivity conditions.

Route speed is an equilibrium outcome: positive demand shocks may increase congestion and lower speeds. I instrument route speed with free-flow speeds during off-peak hours, which primarily reflect permanent infrastructure characteristics (e.g., road capacity, design) rather than contemporaneous demand shocks.

Route distance is determined by network design and depot location and is fixed over the estimation window, so I treat it as exogenous.

Parameter Estimates Table 4 reports the cost parameter estimates. The base labor elasticity parameter γ is estimated at 0.643, indicating that labor requirements scale less than proportionally with vehicle-hours. This relationship suggests the presence of fixed labor components in transit operations, such as supervisory staff or administrative overhead that do not increase one-for-one with service frequency. The magnitude implies that a 10% increase in vehicle-hours translates to approximately a 6.4% increase in labor requirements.

The quality parameter ϕ is estimated at 1.137, reflecting the additional labor costs associated with improving headway regularity. Since regularity enters the cost function as $CV_{rdkt}^{-\phi}$, this positive estimate indicates that reducing the coefficient of variation of headways (improving service quality) requires substantial additional labor inputs. The magnitude suggests that transit operators face steep marginal costs when attempting to provide more regular service, consistent with the intensive monitoring and dispatching efforts required to maintain schedule adherence.

The depot scale parameter ρ is estimated at -0.216, confirming the presence of economies of scale at the depot level. This negative coefficient indicates that routes sharing a common depot benefit from shared resources such as maintenance facilities, supervisory staff, and spare vehicles. The magnitude implies that a 10% increase in the number of routes operated from a depot reduces per-route costs by approximately 2.2%, demonstrating meaningful but modest scale economies in transit operations.

7.3 Road Technology Parameters

I estimate the congestion elasticity η by assuming that $a_{enj} = \log A_{enj} = a_j + \varepsilon_{enj}$. Under this assumption, the estimating equation becomes:

$$\log T_{enj}^{\text{veh}} = \alpha_j + \eta \log V_{en} + \varepsilon_{enj}, \tag{12}$$

where α_j is a mode fixed effect that captures systematic level differences between car and bus travel times. The remaining error ε_{enj} captures unobservable shocks that vary across

periods of the day within edge e.

Parameter Estimates Table 5 presents the road technology parameter estimates. I find elasticities of travel time with respect to traffic flows between 0.12 to 0.13, which are comparable with existing estimates in the literature (Akbar *et al.*, 2023). I also find that buses systematically move at about 70% of car speed along the same edges, regardless of congestion.

7.4 Model Fit

Figure 8 evaluates how well the structural model matches key route-level outcomes in the data. Panel (a) compares predicted and observed ridership and Panel (b) compares predicted and observed route speeds. Observed values are constructed from smart-card boardings and GPS-based speed measures aggregated to the route level.

The model reproduces the rank ordering of routes in both dimensions and tracks the levels reasonably well. For ridership, predicted values explain 56 percent of the cross-sectional variation. Most routes lie close to the 45-degree line, with larger deviations concentrated among a small number of high-ridership routes that exhibit considerable day-to-day variation. This pattern is consistent with the model, which averages over idiosyncratic daily shocks that affect boarding flows.

Route speeds display greater dispersion in the data, reflecting unobserved operational conditions such as temporary congestion bottlenecks, traffic incidents, and within-route heterogeneity in driving behavior. Even so, the model explains 12 percent of the cross-sectional variation and captures the central tendency of speeds across the network. Routes that are systematically slower or faster in the data are similarly positioned in the model, indicating that the congestion technology and route geometry components are reasonably calibrated.

Overall, the model fits the empirical patterns that are most relevant for the counterfactual analysis. It captures how demand responds to service attributes, how operational conditions map into travel speeds, and how these channels combine to generate observed ridership levels. These diagnostics provide confidence that the structural parameters governing traveler behavior, operator choices, and road conditions are suitable for welfare analysis.

8 Counterfactual Simulations

With the structural parameters in hand, I quantify how contract design affects equilibrium prices, service attributes, travel behavior, and welfare. The counterfactual analysis proceeds

in two parts. First, I compare the observed allocation to a set of canonical benchmarks: a welfare-maximizing planner, an unregulated monopoly, and a regulated monopoly. This exercises the demand, supply, and congestion components of the model and clarifies which margins—fares, frequency, or regularity—drive welfare losses under imperfect regulation. Second, I evaluate alternative quality targets by varying the strength of enforcement through the magnitude of the penalties. Third, I study optimal bundling of routes, which determines the effective number of competitors in the procurement auction and, therefore, the extent of market power in contract prices. Taken together, these simulations decompose the welfare consequences of the reform into (i) fare regulation, (ii) quality targets, and (iii) route bundling.

8.1 Baseline Contract Design

Table 6 compares the observed equilibrium (column 1) with three counterfactual regimes. In the baseline, six operators supply bundles of routes under regulated fares and quality targets. Operators receive a per-kilometer compensation determined in a competitive auction, a per-passenger compensation determined by the transit agency, and face monetary penalties for deviations from frequency and CV of headways. Columns 2–4 present counterfactual outcomes under (i) a social planner, (ii) an unregulated monopoly, and (iii) a regulated monopoly. Government transfers to operators are treated as redistributions and are therefore excluded from welfare.

Social Planner Relative to the baseline, the planner lowers the bus fare from \$0.90 to \$0.37 and increases service quality through both higher frequency (+19.5%) and lower dispersion in headways (−20.0% in the CV). Average wait time falls from 5.30 to 4.15 minutes and average speeds increase from 19.1 to 22.2 km/h. These adjustments nearly double transit ridership (from 0.15M to 0.28M trips) and reduce private car trips (from 0.19M to 0.10M). Welfare increases by \$0.55M, primarily due to gains in consumer surplus (\$0.33M) and reductions in environmental externalities (\$0.22M). The decline in externalities is driven by both faster transit speeds and reduced congestion from fewer car trips. Producer surplus is unchanged up to rounding.

Unregulated Monopoly Absent fare regulation and quality targets, the monopoly raises the fare to \$2.11 and reduces service quality (frequency: −29.3%; CV of headways: +39.9%), which increases average wait times (to 8.79 minutes) and reduces speeds (to 16.0 km/h). Transit ridership falls sharply (to 0.07M trips) and private car trips increase (to 0.24M). Because travel times are endogenized through congestion, the mode shift toward driving slows speeds system-wide and raises environmental externalities. Aggregate

welfare decreases by \$0.94M, driven primarily by higher external costs (\$0.85M) and a decline in consumer surplus (\$0.10M). In this scenario, market power operates on both margins—higher fares and degraded service—leading to substantial deadweight loss.

Regulated Monopoly When baseline fares and quality targets are imposed on a monopoly, the equilibrium allocation remains close to the observed outcome: frequency declines modestly (-4.9%), while regularity improves with the CV of headways declining by -8.9%. The small frequency reduction reflects market power in operating decisions: with no competition for passengers, the monopolist finds it profitable to under-provide frequency and incur limited penalties. At the same time, unified network control slightly improves regularity through better coordination across routes. Transit and private car trips are nearly identical to baseline, and welfare differences are numerically negligible. The main difference relative to column (1) is fiscal: the monopolist extracts a higher per-kilometer contract price in the procurement stage, which does not affect total welfare in the benchmark accounting because transfers are distributional.

Overall, the results highlight the central role of quality regulation. In its absence, monopoly power generates higher fares, degraded service, congestion, and large external costs. When fares and quality are regulated, a single supplier replicates the user-side allocation and exercises market power primarily through fiscal channels rather than reduced service quality.

8.2 Optimal Quality Targets

The descriptive evidence in Section 5 shows that operators consistently met frequency targets but often deviated from regularity targets in the pre-reform period. This pattern suggests that the penalty on frequency deviations was strong enough to induce compliance, while the penalty associated with wait-time deviations, which internalizes both frequency and regularity, was too weak to affect dispatching behavior. Taken together, the evidence indicates that enforcement strength is an important margin through which contract design affects service quality. In this subsection, I use the structural model to evaluate how stronger enforcement of the wait-time component of the contract affects operator choices, travel behavior, and welfare.

The analysis proceeds in two steps. First, I solve the social planner's problem under the baseline route bundle design and fare structure. The planner chooses route-level frequency and regularity to maximize welfare, taking prices and network structure as given. I use the resulting planner-optimal service attributes as the quality targets in the counterfactual scenario. These targets reflect the levels of frequency and regularity that would be socially optimal in the current institutional environment.

Second, I evaluate the penalty strength needed to induce firms to meet these targets. To reduce computational burden, and consistent with the descriptive evidence, I treat the current penalty on frequency deviations as sufficiently calibrated. I then search for the system-wide wait time penalty τ^w that maximizes welfare when firms choose service attributes in response to the planner's target levels. All other components of the contract remain fixed at their baseline values, including fare regulation, route bundling, and the per-kilometer payments determined in the procurement auctions.

Figure 9 presents the results. The welfare-maximizing wait time penalty is τ^{w*} = \$85 per minute of deviation from the target wait time. Increasing the strength of this penalty leads firms to provide more regular service and slightly higher frequency, which reduces average wait times, increases transit ridership, and modestly decreases private vehicle trips. These adjustments generate welfare gains of approximately \$0.1 million in the morning peak period relative to the current equilibrium. The gains arise primarily from reduced waiting times, with only small changes in external costs.

This exercise shows that stronger enforcement of regularity yields meaningful improvements in service quality and welfare. The frequency penalty already induces compliance, but the regularity component of the contract remains too weak to align firm behavior with the socially desired level of headway consistency. Strengthening the wait time penalty closes a nontrivial portion of the welfare gap between the observed allocation and the planner's optimum, without altering fares, network structure, or market power in the procurement stage.

9 Conclusion

Contract design in public transit must correct two coexisting distortions: market power, which leads firms to underprovide service quality, and uninternalized network effects, which fragment coordination across routes. These forces pull in opposite directions, as competition curbs market power but weakens coordination, making it difficult for regulators to achieve efficient and reliable service. Because these contracts shape both welfare and environmental outcomes through their effects on ridership and congestion, understanding how to balance these distortions is central to effective public transit design.

This paper combines quasi-experimental evidence to document how the contractual instruments—quality targets and route bundling—interact with these distortions, and a structural model to quantify their social welfare implications. Linking household travel surveys, smart-card transactions, and high-frequency GPS data, I use a difference-in-differences design to show that stricter quality targets improve service quality while awarding more bundles to independent operators fragments the network and weakens

coordination. To quantify the welfare implications of these effects and test alternative contract designs, I estimate a structural model of demand, supply, and congestion that captures network effects through route complementarities.

In the absence of regulatory intervention, consumer surplus follows an inverted-U pattern as competition increases: entry initially improves welfare by reducing markups, but excessive fragmentation erodes coordination, degrading reliability and increasing congestion. Stricter quality targets help offset these coordination losses by aligning service decisions more closely with social benefits and pulling externalities toward their efficient level. These results show that effective contract design must balance competition and coordination rather than maximizing either in isolation.

A common regulatory approach treats quality standards and market structure as independent levers, tightening one while holding the other fixed. The results here show that in network industries, these instruments are interdependent: the degree of route consolidation determines how effectively quality targets translate into improvements in service quality and welfare. Because any reform inevitably affects both competition and coordination, contract design should explicitly integrate these channels. A joint approach, in which quality incentives are calibrated to the network structure they operate within, can achieve substantially higher welfare than policies that adjust targets or bundling in isolation.

This analysis focuses on how contractual instruments shape short-run operational choices, taking the tendering stage as given. A natural extension would examine the design of scoring auctions that allocate routes and determine entry, exploring whether alternative scoring rules or bundling criteria could improve the balance between competition and coordination. Another important direction is to study how collusion, contract renegotiation, or dynamic investment decisions in capital such as buses and depots affect regulatory effectiveness once operations begin. Extending the framework to integrate procurement and regulation would deepen our understanding of how these stages jointly shape outcomes in network industries with private provision.

More broadly, the findings illustrate that effective regulation in networked public services depends not only on reducing costs or promoting competition, but also on ensuring that decentralized decisions align with systemwide efficiency. As governments worldwide restructure transit, electricity, and telecommunications networks, understanding how to jointly design incentives and market structure becomes essential. Developing empirical tools to quantify how private incentives diverge from social optima and to inform the design of regulation where market failures coexist offers a rich agenda for future research.

References

Akbar, P., Couture, V., Duranton, G. and Storeygard, A. (2023). Mobility and Congestion in Urban India. *American Economic Review*, **113** (4), 1083–1111.

Almagro, M., Barbieri, F., Castillo, J. C., Hickok, N. and Salz, T. (2022). *Optimal Urban Transportation Policy: Evidence from Chicago*. Working paper.

Bajari, P., Houghton, S. and Tadelis, S. (2014). Bidding for Incomplete Contracts: An Empirical Analysis of Adaptation Costs. *American Economic Review*, **104** (4), 1288–1319.

— and Tadelis, S. (2001). Incentives versus Transaction Costs: A Theory of Procurement Contracts. *RAND Journal of Economics*, pp. 387–407.

Barwick, P. J., Kwon, H.-S. and Li, S. (2024a). *Attribute-based Subsidies and Market Power: an Application to Electric Vehicles*. Working Paper 32264, National Bureau of Economic Research.

—, Li, S., Waxman, A., Wu, J. and Xia, T. (2024b). Efficiency and Equity Impacts of Urban Transportation Policies with Equilibrium Sorting. *American Economic Review*, **114** (10), 3161–3205.

Björkegren, D., Duhaut, A., Nagpal, G. and Tsivanidis, N. (2025). *Public and Private Transit: Evidence from Lagos*. Working Paper 33899, National Bureau of Economic Research.

Bordeu, O. (2023). *Commuting Infrastructure in Fragmented Cities*. Working paper.

Bosio, E., Djankov, S., Glaeser, E. and Shleifer, A. (2022). Public Procurement in Law and Practice. *American Economic Review*, **112** (4), 1091–1117.

Brancaccio, G., Kalouptsidi, M. and Papageorgiou, T. (2020). Geography, Transportation, and Endogenous Trade Costs. *Econometrica*, **88** (2), 657–691.

—, —, — and Rosaia, N. (2023). Search Frictions and Efficiency in Decentralized Transport Markets. *The Quarterly Journal of Economics*, **138** (4), 2451–2503.

Buchholz, N. (2022). Spatial Equilibrium, Search Frictions, and Dynamic Efficiency in the Taxi Industry. *The Review of Economic Studies*, **89** (2), 556–591.

Castillo, J. C. (2025). Who Benefits from Surge Pricing? *Econometrica*, **93** (5), 1811–1854.

CEDEUS (2024). Encuesta de Movilidad de Santiago 2024. Accessed October 2025.

Chen, Y. (2024). *Network Structure and the Efficiency Gains from Mergers: Evidence from US Freight Railroads*. Working paper.

Ciliberto, F., Murry, C. and Tamer, E. (2021). Market Structure and Competition in Airline Markets. *Journal of Political Economy*, **129** (11), 2995–3038.

Conwell, L. (2023). *Subways or Minibuses? Privatized Provision of Public Transit*. Working paper.

Degiovanni, P. and Yang, R. Y. (2023). *Economies of Scale and Scope in Railroading*. Working paper.

DIPRES (2022). *Programas Presupuestarios 2022*. Tech. rep., Ministerio de Hacienda, Gobierno de Chile.

DTPM (2022). *Memoria Anual 2022*. Tech. rep., Ministerio de Transportes y Telecomunicaciones, Gobierno de Chile.

Duggan, M. G. (2000). Hospital Ownership and Public Medical Spending. *The Quarterly Journal of Economics*, **115** (4), 1343–1373.

Economides, N. (1996). The Economics of Networks. *International Journal of Industrial Organization*, **14** (6), 673–699.

Frechette, G. R., Lizzeri, A. and Salz, T. (2019). Frictions in a Competitive, Regulated Market: Evidence from Taxis. *American Economic Review*, **109** (8), 2954–2992.

Gagnepain, P. and Ivaldi, M. (2002). Incentive Regulatory Policies: The Case of Public Transit Systems in France. *RAND Journal of Economics*, pp. 605–629.

Galiani, S., Gertler, P. and Schargrodsky, E. (2005). Water for Life: The Impact of the Privatization of Water Services on Child Mortality. *Journal of Political Economy*, **113** (1), 83–120.

Harris, A. and Yellen, M. (2024). *Decision-Making with Machine Prediction: Evidence from Predictive Maintenance in Trucking*. Working paper.

Hart, O., Shleifer, A. and Vishny, R. W. (1997). The Proper Scope of Government: Theory and an Application to Prisons. *The Quarterly Journal of Economics*, **112** (4), 1127–1161.

Jerch, R., Kahn, M. E. and Li, S. (2017). The Efficiency of Local government: The Role of Privatization and Public Sector Unions. *Journal of Public Economics*, **154**, 95–121.

Kelley, E. M., Lane, G. and Schönholzer, D. (2024). Monitoring in Small Firms: Experimental Evidence from Kenyan Public Transit. *American Economic Review*, **114** (10), 3119–3160.

Kreindler, G., Gaduh, A., Graff, T., Hanna, R. and Olken, B. A. (2023). *Optimal Public Transportation Networks: Evidence from the World's Largest Bus Rapid Transit System in Jakarta*. Working Paper 31369, National Bureau of Economic Research.

Levin, J. and Tadelis, S. (2010). Contracting for Government Services: Theory and Evidence from US Cities. *The Journal of Industrial Economics*, **58** (3), 507–541.

Lewis, G. and Bajari, P. (2011). Procurement Contracting with Time Incentives: Theory and Evidence. *The Quarterly Journal of Economics*, **126** (3), 1173–1211.

— and — (2014). Moral Hazard, Incentive Contracts, and Risk: Evidence from Procurement. *Review of Economic Studies*, **81** (3), 1201–1228.

Marra, M. and Oswald, F. (2023). *Spatial Rents, Garage Location, and Competition in the London Bus Market*. Working paper.

Mbonu, O. and Eaglin, F. C. (2024). *Market Segmentation and Coordination Costs: Evidence from Johannesburg's Minibus Networks*. Working paper.

Munizaga, M. A. and Palma, C. (2012). Estimation of a Disaggregate Multimodal Public Transport Origin–Destination Matrix from Passive Smartcard Data from Santiago, Chile. *Transportation Research Part C: Emerging Technologies*, **24**, 9–18.

Parry, I. W. H. and Small, K. A. (2009). Should Urban Transit Subsidies be Reduced? *American Economic Review*, **99** (3), 700–724.

Rosaia, N. (2025). Competing Platforms and Transport Equilibrium. *Econometrica*, Forthcoming.

Spence, A. M. (1975). Monopoly, Quality, and Regulation. *The Bell Journal of Economics*, pp. 417–429.

Tsivanidis, N. (2025). Evaluating the Impact of Urban Transit Infrastructure: Evidence from Bogota's Transmilenio. *American Economic Review*, Forthcoming.

Wang, B. (2024). *Public Transit Provision and Fare Structure in U.S. Cities*. Tech. rep.

Wolfram, C., Miguel, E., Hsu, E. and Berkouwer, S. B. (2023). *Donor Contracting Conditions and Public Procurement: Causal Evidence from Kenyan Electrification*. Working Paper 30948, National Bureau of Economic Research.

Yuan, Z. and Barwick, P. J. (2024). *Network Competition in the Airline Industry: An Empirical Framework*. Working Paper 32893, National Bureau of Economic Research.

Tables and Figures

Table 1: Effect of Network Fragmentation on Service Attributes

	Log Frequency (1)	Log CV of Headways (2)	Log Wait Time (3)
Log Concentration (HHI)	-0.159***	-0.244***	-0.023***
	(0.009)	(0.010)	(0.005)
Covariates	✓	✓	✓
Origin-Destination FEs	✓	✓	✓
Date FEs	✓	✓	✓
Trip FEs	✓	✓	✓
Observations	8,061,997	8,061,997	8,061,997
Within R^2	0.821	0.617	0.285

Notes: This table reports regression estimates of the relationship between network concentration and service quality. The unit of observation is a trip–origin–destination choice set on a given date. Origin-destination pairs and trip characteristics are derived from the 2012-2013 household travel survey, while service attributes (frequency, headway regularity, wait times) are constructed from observed transit operations during August to December 2022. The dependent variables are the log of aggregate frequency, the log of the coefficient of variation of headways, and the log of expected wait time. The variable of interest is the log of the Herfindahl–Hirschman Index (HHI), constructed from route-level market shares based on planned frequencies. All regressions control for the total planned frequency and the number of routes in the market. Origin-destination, date, and trip fixed effects are included, and standard errors are clustered at the traveler level. *** $p < 0.01$, ** $p < 0.05$, * $p < 0.1$.

Table 2: Effect of Stricter Quality Targets on Service Attributes and Ridership (DiD Estimates)

	Log Frequency			Log CV of Headways			Log Wait Time			Log Ridership		
	(1)	(2)	(3)	(4)	(5)	(6)	(7)	(8)	(9)	(10)	(11)	(12)
Treated	0.004	0.039*	0.027	-0.312***	-0.196**	-0.165**	-0.060**	-0.096**	-0.088**	0.156	0.139*	0.117**
	(0.039)	(0.018)	(0.016)	(0.039)	(0.053)	(0.044)	(0.015)	(0.029)	(0.030)	(0.115)	(0.064)	(0.035)
Covariates	✓	✓	✓	✓	✓	✓	✓	✓	✓	✓	✓	✓
Route FEs		✓	✓		✓	✓		✓	✓		✓	✓
Date FEs		✓	✓		✓	✓		✓	✓		✓	✓
Firm FEs			✓			✓			✓			✓
Observations	69,296	69,296	69,296	69,296	69,296	69,296	69,296	69,296	69,296	69,234	69,234	69,234
Within R^2		0.700	0.702		0.076	0.060		0.088	0.069		0.230	0.238

Notes: This table reports difference-in-differences regression estimates of the effect of stricter quality targets on service attributes and ridership. The unit of observation is a route on a given date, and the sample is restricted to departures monitored at the start control point. Observed frequency, headway regularity (measured as the coefficient of variation of headways), expected wait time, and daily ridership are constructed from GPS and smart-card data from August 2022 to August 2023. The dependent variables are the logarithm of observed frequency, the logarithm of the coefficient of variation of headways, the logarithm of expected wait time, and the logarithm of total ridership. The variable of interest is *Treated*, an indicator equal to one when a route-date observation is subject to stricter quality targets and zero otherwise. All regressions control for planned frequency, planned regularity (planned CV), and route distance. Columns (2), (5), (8), and (11) include route and date fixed effects, and columns (3), (6), (9), and (12) additionally include firm fixed effects. Standard errors are clustered at the stable-firm level. *** $p < 0.01$, ** $p < 0.05$, * $p < 0.10$.

Table 3: Travel Preference Parameters

	(1)	(2)	(3)	(4)
Wait time (hr)	-8.077***	-8.394***	-8.368***	-8.356***
	(0.139)	(0.148)	(0.149)	(0.148)
Travel time (hr)	-4.585***	-4.620***	-4.763***	-4.655***
	(0.080)	(0.082)	(0.084)	(0.080)
Cost ($)	-0.410***	-0.412***	-0.416***	-0.424***
	(0.015)	(0.015)	(0.016)	(0.015)
Transfer penalty	-0.954***	-0.985***	-0.988***	-0.979***
	(0.022)	(0.023)	(0.023)	(0.026)
Random coefficients on mode dummies (σ_j)				
Car				0.628***
				(0.068)
Transit				0.848***
				(0.090)
Mode FE	Yes	Yes	Yes	Yes
Mode × Trip Related FE	No	Yes	Yes	Yes
Mode × Demographics FE	No	No	Yes	Yes
Log-likelihood	-50932.6	-50814.0	-48557.7	-48331.6
Mean VOT ($/hr)	11.2	11.2	11.4	10.9
Observations	49,157	49,157	49,157	49,157

Notes: This table reports travel preference parameter estimation results from the specifications outlined in section 7.1. The estimation sample is based on the full set of trips. The parameters are estimated via MLE. VOT stands for value of time measure in dollar per hour. Mode-Trip related fixed effects include trip distance, purpose, time period, and CBD origin/destination indicators. Mode-Demographics fixed effects include education, age, and gender. Standard errors in parentheses. *** $p < 0.01$, ** $p < 0.05$, * $p < 0.1$.

Table 4: Cost Parameters

	(1)
Base Labor (γ)	0.643***
	(0.058)
Quality (ϕ)	1.137***
	(0.015)
Depot scale (ρ)	-0.216***
	(0.052)
Observations	152,883

Notes: This table reports GMM estimates of the cost parameters from Equation 9. The parameter γ governs how operating costs vary with service frequency, ϕ captures the cost consequences of headway regularity, and ρ measures depot-level scale effects. The estimation uses route–day observations and instruments based on unexpected operational shocks, reform-driven changes in quality targets, and depot reallocations. Standard errors are clustered at the firm level. *** $p < 0.01$, ** $p < 0.05$, * $p < 0.1$.

Table 5: Road Technology Parameters

	Log Travel Time		
	(1)	(2)	(3)
Car Constant	-0.361***	-0.400***	-0.400***
	(0.077)	(0.084)	(0.084)
Log Traffic Flow	0.130*	0.124***	0.119**
	(0.061)	(0.037)	(0.036)
Monitoring Station FEs		X	X
Date FEs			X
Observations	70,174	70,174	70,174
Within R^2		0.128	0.128

Notes: This table reports regression estimates of the relationship between traffic flow and travel times. The unit of observation is a traffic monitoring station, measured in 15-minute intervals between 6am and 9pm. The dependent variable is the log of travel time (in hours) for the corresponding road segment. The independent variable is the log of vehicle flows, measured in vehicles per hour. The regression is pooled across cars and buses, with a mode-specific constant capturing systematic differences in travel times between modes. The sample covers 64 traffic monitoring stations across 9 municipalities and is restricted to cases where flow per lane is below 1,100 vehicles per hour. This threshold corresponds to the maximum capacity of a lane in urban areas with intersections and traffic lights and retains 99.4% of the observations. Standard errors are clustered at the municipality level. *** $p < 0.01$, ** $p < 0.05$, * $p < 0.1$.

Table 6: Counterfactual Results Under Alternative Market Structures and Regulatory Constraints (Relative to Baseline)

	Baseline (1)	Social Planner (2)	Monopoly (U) (3)	Monopoly (R) (4)
Panel A: Prices				
Bus Price ($)	0.90	0.37	2.11	0.90
Bus $\rightarrow$ Metro Transfer Price ($)	0.10	0.13	0.10	0.10
Panel B: Service Attributes				
Δ Frequency (%)	0.00%	19.50%	-29.26%	-4.88%
Δ CV of Headways (%)	0.00%	-19.96%	39.93%	-8.98%
Avg. Wait (min)	5.30	4.15	8.79	5.41
Avg. Speed (km/h)	19.06	22.20	16.01	19.06
Panel C: Trips				
Transit (M)	0.15	0.28	0.07	0.15
Private Car (M)	0.19	0.10	0.24	0.19
Panel D: Welfare				
Δ Welfare (M)	0.00	0.54	-0.94	-0.00
Δ Consumer Surplus (M)	0.00	0.33	-0.10	-0.00
Δ Producer Surplus (M)	0.00	-0.00	0.00	0.00
Δ Externalities (M)	0.00	-0.22	0.85	0.00

Notes: Column (1) reports the observed allocation under regulated fares and quality targets with six operators. Column (2) shows the welfare-maximizing allocation chosen by a social planner. Column (3) corresponds to an unregulated monopoly that selects fares and service attributes to maximize profits. Column (4) imposes the same fare regulation and quality targets as in the baseline on a monopolist. Δ Frequency and Δ CV of Headways report percentage changes relative to the baseline. Lower CV of headways values denote more regular service. Welfare is measured as the sum of consumer surplus, producer surplus, and environmental externalities, and is normalized to zero in the baseline. Government transfers to operators are treated as internal redistributions and therefore do not enter the welfare measure. "M" denotes millions.

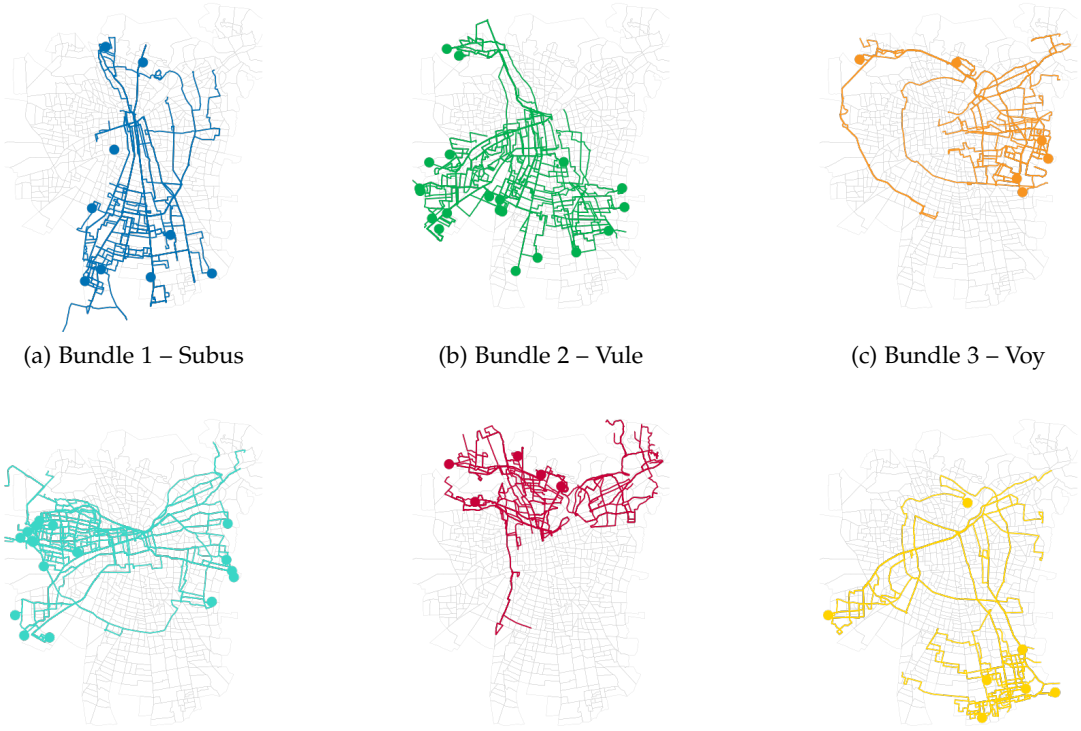

(a) Bundle 1 – Subus (b) Bundle 2 – Vule (c) Bundle 3 – Voy

(d) Bundle 4 – Metbus (e) Bundle 5 – Redbus (f) Bundle 6 – STP

Figure 1: Route Bundles and Depot Locations.

Notes: The figure shows the route bundles operated by each firm in August 2022. A route bundle refers to the group of routes assigned to a given operator. Colored lines trace the individual routes within each bundle, and filled circles indicate the depots from which those routes are dispatched and operated.

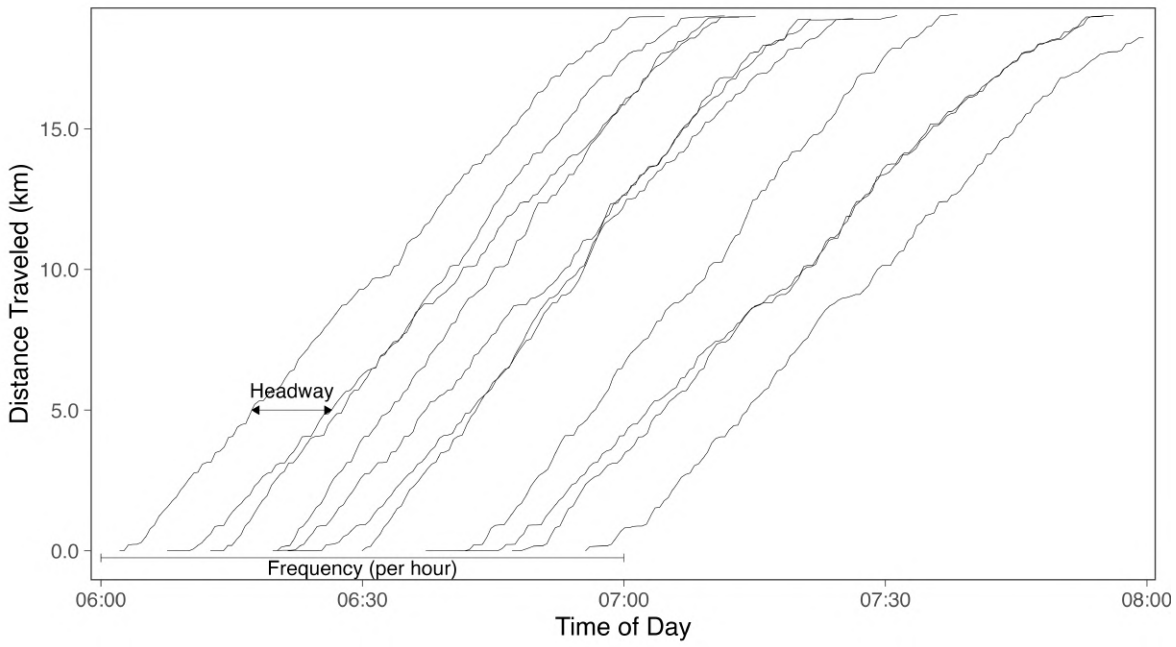

Figure 2: GPS-Based Bus Trajectories and Service Attributes.

Notes: The figure plots GPS trajectories for buses operating on one example route over a one-hour period. Each line corresponds to a single bus dispatch and shows the distance traveled over time. The number of dispatches within this period reflects the route's frequency, which I report in buses per hour. The time gap between consecutive buses is the headway, and the consistency of these intervals determines the regularity of service. I measure regularity using the coefficient of variation of headways within each monitoring period. Both frequency and regularity shape traveler wait times and are directly incentivized by the contract's quality targets.

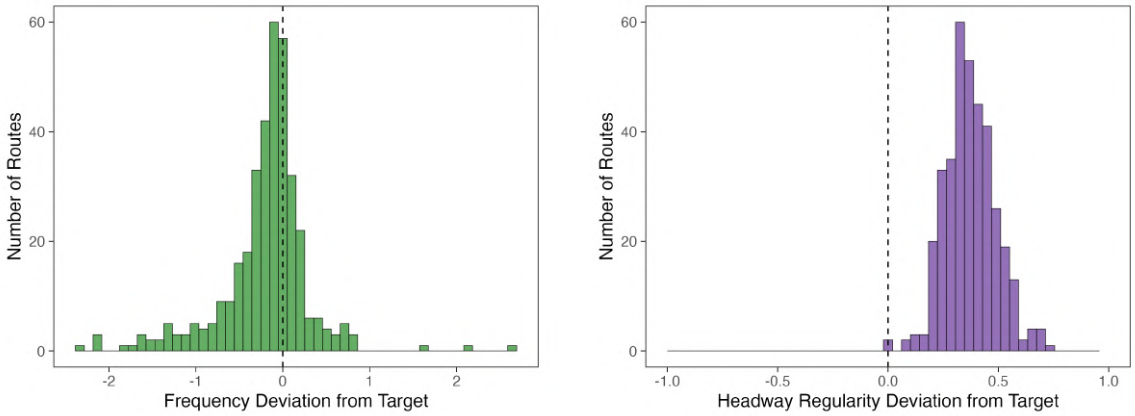

(a) Frequency

(b) Headway Regularity

Figure 3: Distribution of Deviations from Planned Service Attributes (Pre-Reform Period).

Notes: This figure shows the distribution of deviations between planned and observed service attributes across routes during the pre-reform period. The unit of observation is a route, and deviations are constructed by averaging observed service attributes over all pre-reform operating days. Panel (a) plots deviations in frequency, defined as planned frequency minus observed frequency. Panel (b) plots deviations in regularity, defined as observed minus planned headway regularity (measured using the coefficient of variation of headways). Planned service attributes are obtained from operator quality targets, and observed attributes are constructed from GPS data. The vertical dashed line at zero represents full adherence to planned service levels.

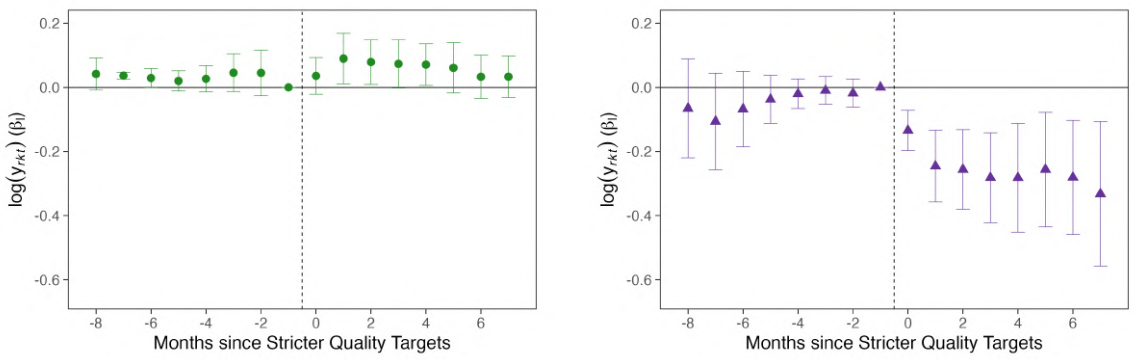

(a) Frequency

(b) Headway Regularity

Figure 4: Event-Study Estimates of the Effect of Stricter Quality Targets on Service Attributes.

Notes: This figure reports event-study estimates of the effect of stricter quality targets on transit service attributes. Time is measured in months relative to each route's implementation date, with the month prior to treatment serving as the omitted category. The unit of observation is a route on a given date, and the sample is restricted to departures monitored at the start control point. The dependent variables are the logarithm of observed frequency (Panel a) and the logarithm of the coefficient of variation of headways (Panel b), both constructed from GPS data from August 2022 to August 2023. Each specification controls for planned frequency, planned regularity (planned CV), and route distance, and includes route, firm, and date fixed effects. Points report the estimated event-time coefficients and vertical bars show 95 percent confidence intervals. Standard errors are clustered at the stable-firm level.

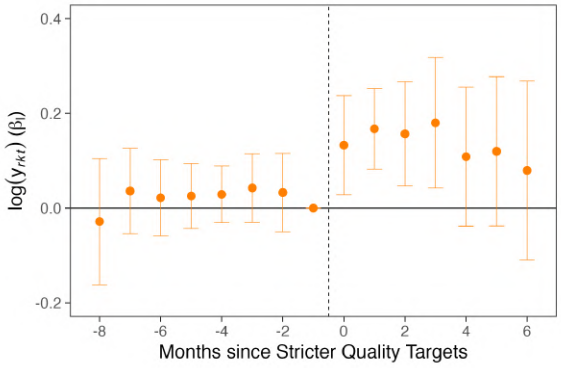

Figure 5: Event-Study Estimates of the Effect of Stricter Quality Targets on Ridership.

Notes: This figure reports event-study estimates of the effect of stricter quality targets on passenger ridership. Time is measured in months relative to each route's implementation date, with the month prior to treatment serving as the omitted category. The unit of observation is a route on a given date. The dependent variable is the logarithm of total ridership, constructed from smart-card validations between August 2022 and August 2023. The specification controls for planned frequency, planned regularity (planned CV), and route distance, and includes route, firm, and date fixed effects. Points report the estimated event-time coefficients and vertical bars show 95 percent confidence intervals. Standard errors are clustered at the stable-firm level.

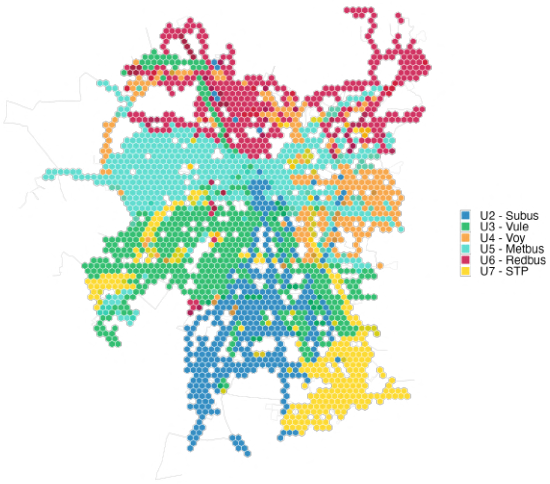

(a) Pre-reform Transit Firm Dominance in 2022
(6 bundles and 6 firms)

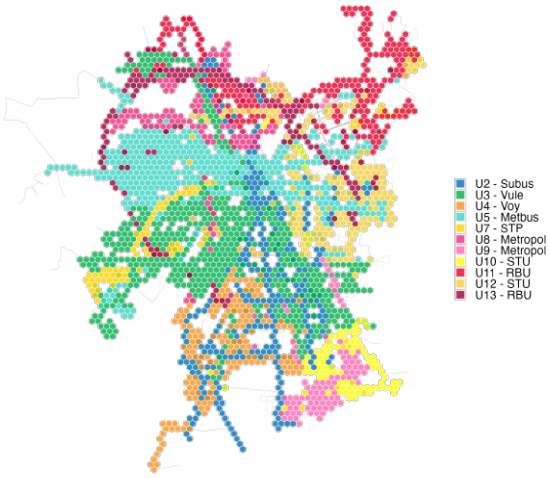

(b) Post-reform Transit Firm Dominance in 2023
(11 bundles and 8 firms)

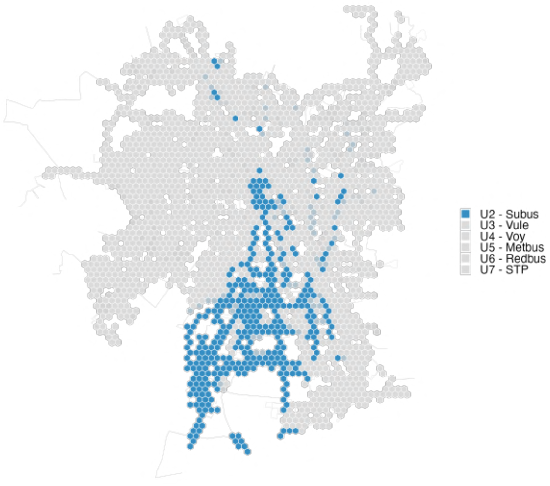

(c) Pre-Reform Southern Network, August 2022

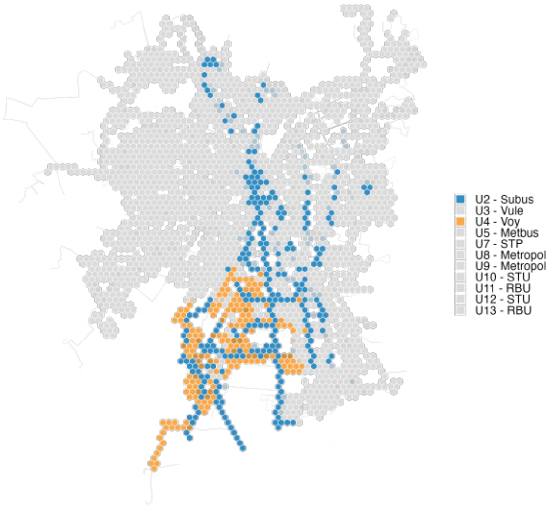

(d) Pre-Reform Southern Network, December 2022

Figure 6: Transit Network Fragmentation.

Notes: The figures display transit network fragmentation using a hexagonal grid of geographic firm dominance. Panel (a) shows the network before the contract reform, and Panel (b) shows it after the reform, which both reallocated routes and introduced stricter quality targets for about 40% of the system. Panels (c) and (d) instead show a pre-reform rebundling that reallocated some routes without changing quality targets, isolating the effect of rebundling alone. Panel (c) shows August 2022, when a single firm dominated the south, while Panel (d) shows December 2022, when two firms shared that area. Each hexagon marks a location where one firm operates the plurality of routes and has more than 25% local share, with a minimum of three routes. Colors indicate operators; blank areas have insufficient density or no dominant firm.

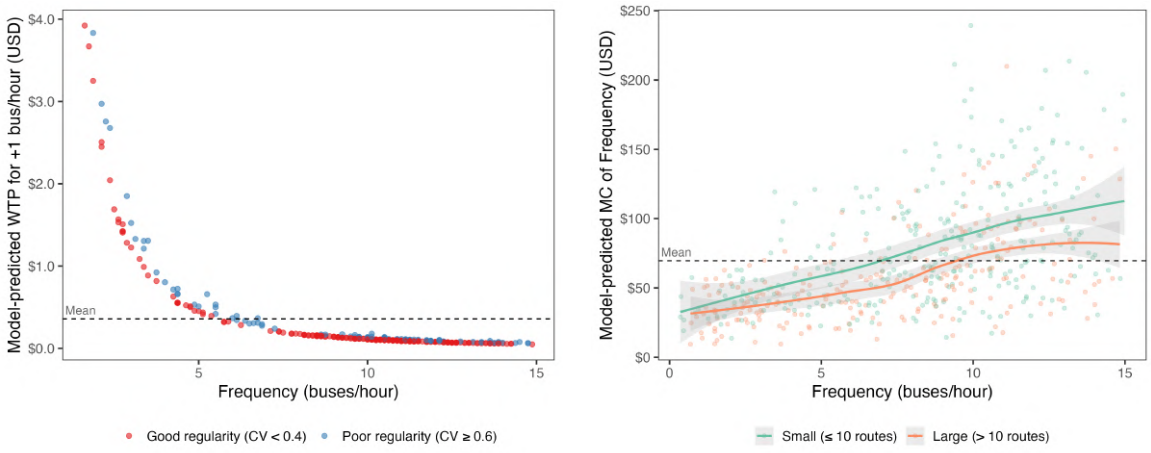

(a) Willingness to Pay for Frequency

(b) Marginal Cost of Frequency

Figure 7: Frequency - Demand and Supply

Notes: The figure summarizes how estimated preferences and cost parameters translate into the willingness to pay (WTP) and marginal cost (MC) of frequency. Panel (a) displays the willingness to pay, computed from demand-side preference estimates for waiting time, as frequency increases. Routes are grouped by service regularity: those with low coefficients of variation of headways (regular service), shown in red, and those with high coefficients of variation (irregular service), shown in blue. Panel (b) shows the marginal cost of frequency, computed from supply-side cost parameters, as frequency increases. Routes are grouped by depot load: those operated from depots with fewer than ten routes (low load), shown in green, and those with more than ten routes (high load), shown in orange.

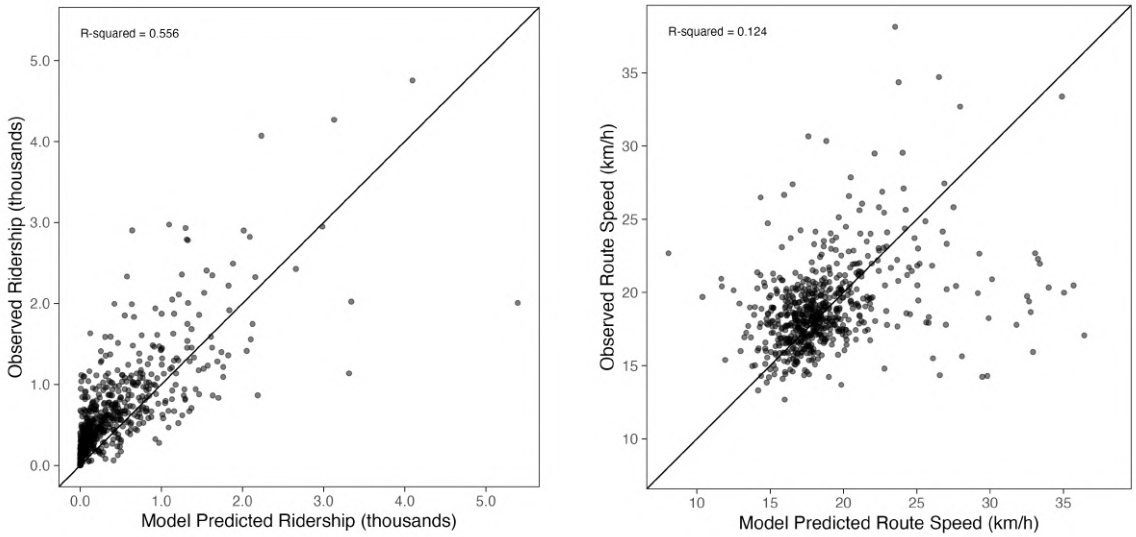

(a) Ridership

(b) Route Speed

Figure 8: Model Fit

Notes: This figure compares model predictions and observed data on bus operations. Panel (a) compares model predictions of route-level ridership to observed ridership from the smart-card validation data. Panel (b) compares model predictions of average route speeds to observed speeds computed from GPS bus location records. In both panels, observed values are constructed directly from administrative data, while predicted values are generated by the model described in Section 6 using the parameter estimates from Section 7.

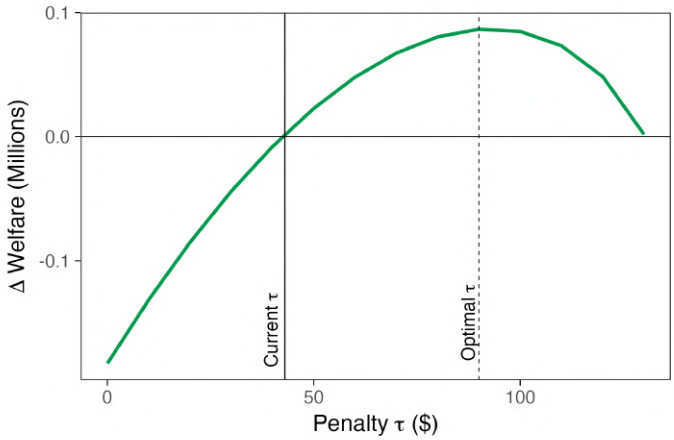

Figure 9: Optimal Quality Targets: Welfare Effects of the Wait Time Penalty.

Notes: This figure plots the welfare change in the morning peak period relative to the current equilibrium as a function of the wait time penalty parameter τ. The solid green line reports the welfare difference evaluated at each penalty level, holding all other components of the contract fixed at their baseline values. Welfare is computed using the structural model, allowing operator choices of frequency and regularity, traveler route choices, and congestion effects to adjust to the implied service attributes. The vertical solid line marks the current penalty level used in the contract. The vertical dashed line marks the welfare-maximizing penalty τ^{w*}, which equals \$85 per minute of deviation from the target wait time..

Appendix A Data Sources

Santiago Household Travel Survey (SHTS) Data

The Santiago Household Travel Survey (SHTS) was designed using the Smith method to ensure sufficient sample size at the municipality level for estimating trip generation rates, modal shares, and car ownership rates. Within each municipality, blocks were selected using probability proportional to size (PPS) sampling with replacement. A minimum of 160 households were surveyed in each municipality, with 100 interviews on weekdays and 60 on weekends.

The final survey sample includes 18,264 households: 11,246 interviewed on weekdays during the regular season and 7,018 interviewed on weekends across both regular and summer seasons. Data collection during the regular season took place between July 2012 and November 2013, and during the summer season in January and February of 2013.

Interviews were conducted in person using mobile devices and followed a two-visit protocol. During the first visit, surveyors introduced the study, collected household characteristics, and assigned a random travel day for each household member. Respondents received a travel diary to record their trips. In the second visit, surveyors completed in-person interviews for each member to retrieve trip data; if a respondent was unavailable, the surveyor returned. This procedure reduces trip underreporting relative to single-visit or recall-only surveys.

The SHTS provides rich information on individuals (age, gender, number of trips, driver license, education, occupation, and income), households (georeferenced location, household size, number of vehicles, tenure, and income), and trips (georeferenced origins and destinations, purpose, mode, travel time, and time of day).

I restrict the data to the urban area of Santiago, yielding 13,696 households, 31,735 travelers, and 74,166 trips. I then apply the following sample restrictions. I drop trips using modes other than car, public transit, or walking (15.73%); observations with purposes outside work, study, or other (0.38%); observations with implausible distances or travel times (0.43%); trips with missing income (0.44%); and incomplete cases (0.01%). The resulting sample contains 12,668 households, 27,111 travelers, and 61,574 trips. Considering weekdays only to focus on regular commuting patterns, the resulting estimation sample contains 11,612 households, 22,653 travelers, and 47,622 trips.

Monetary costs vary by mode. Walking is costless. Public transit fares are flat for buses (1.1 USD) and period-dependent for the subway (1.3 USD in peak and 1.2 USD in off-peak). Transfers are free within 1.5 hours except between bus and subway, which require a small subway co-payment. High school students travel for free and university students pay a discounted fare of 0.4 USD. For car users, I compute fuel costs using an average fuel

consumption of 0.11 liters/km (9 km/liter) from the *Ministerio de Energía* and a gasoline price of 1.61 USD/liter.

Appendix B Model Estimation

This appendix provides additional detail on the estimation of the structural model. I begin by outlining the estimation of traveler preference parameters on the demand side, followed by the estimation of cost parameters on the supply side. Together, these estimates discipline the equilibrium outcomes in the model.

Appendix B.1 Travel Preference Parameters

I estimate travel preferences using a two-stage discrete choice model explained in Section 6.1. Travelers first choose a transportation mode (car, public transit, or outside option), then conditional on choosing transit, they select a specific route. I estimate this model by Simulated Maximum Likelihood using 100 Halton draws.

Stage 2: Transit Route Choice Consider an origin–destination market m with transit options $h \in \mathcal{H}_m$ (direct or single-transfer routes). Each option delivers utility

$$u_h = v_h + \alpha_{\text{wait}} T_h^{\text{wait}},$$

where v_h is the deterministic component and $T_h^{\text{wait}} \sim \text{Exp}(\lambda_h)$ is random waiting time arising from Poisson arrivals. Following Kreindler *et al.* (2023), this yields closed-form route choice probabilities

$$\pi_h = P(h \mid \text{transit}, m; \alpha_{\text{wait}}, \lambda, v)$$

and an inclusive value summarizing transit attractiveness:

$$I_m \equiv \mathbb{E} \max_{h \in \mathcal{H}_m} u_h. \tag{13}$$

Stage 1: Mode Choice At the mode choice stage, traveler i in market m receives utility from mode j:

$$U_{ijm} = \theta_{ij} + v_{jm} + \varepsilon_{ijm}, \tag{14}$$

where $\theta_{ij} \sim \mathcal{N}(\bar{\theta}_j, \sigma_j^2)$ is a random coefficient capturing unobserved preference heterogeneity, v_{jm} is the deterministic utility (with $v_{\text{transit},m} = I_m$ from equation (13)), and ε_{ijm} is i.i.d.

Type I extreme value.

This yields a mixed logit probability, approximated by simulation with R Halton draws:

$$P(j_i \mid m_i) \approx \frac{1}{R} \sum_{r=1}^{R} \frac{\exp(U_{ijm}^{(r)})}{\sum_k \exp(U_{ikm}^{(r)})}, \tag{15}$$

where $U_{ijm}^{(r)}$ evaluates (14) at draw r.

Likelihood Function The individual contribution to the likelihood combines both stages. Let j_i denote i's chosen mode and h_i the chosen route when $j_i = \text{transit}$. Then:

$$L_i = P(j_i \mid m_i) \times \pi_{h_i}^{\mathbf{1}\{j_i = \text{transit}\}}, \tag{16}$$

and the log-likelihood is

$$\ln \mathcal{L} = \sum_i \left[\ln P(j_i \mid m_i) + \mathbf{1}\{j_i = \text{transit}\} \ln \pi_{h_i} \right]. \tag{17}$$

Relationship to nested logit. This structure resembles a nested logit but differs in two ways: (i) route choice probabilities arise from exponential waiting-time shocks rather than GEV structure, and (ii) the mode choice stage includes random coefficients. Substitution across routes is governed by α_{wait} and frequency λ_h, while cross-mode substitution is captured by $\{\bar{\theta}_j, \sigma_j^2\}$.

Appendix B.2 Cost Parameters

This subsection provides additional detail on the estimation of the structural cost parameters. The route-level cost function is derived in Section 6.2. Here, I focus on the marginal cost expressions, the econometric specification, and the GMM procedure used to estimate the cost parameters.

Route-Level Cost Function Operational costs on route r, at depot d, for firm k at time t are:

$$C_{rdkt} = w_k \cdot \left(f_{rdkt} \cdot \frac{L_r^T}{s_{rt}} \right)^{\gamma} \cdot CV_{rdkt}^{-\phi} \cdot |\mathcal{R}_{dkt}|^{\rho} \cdot \varepsilon_{rdkt},$$

where w_k is the wage rate, γ governs the elasticity of labor demand with respect to vehicle-hours, ϕ captures the additional labor effort required to improve regularity, ρ captures depot-level scale effects, and ε_{rdkt} is a route-level productivity shock.

Marginal Costs Differentiating the cost function yields the marginal cost of frequency and regularity:

$$\frac{\partial C_{rdkt}}{\partial f_{rdkt}} = w_k \cdot \gamma \cdot \left(f_{rdkt} \cdot \frac{L_r^T}{s_{rt}} \right)^{\gamma - 1} \cdot \left(\frac{L_r^T}{s_{rt}} \right) \cdot CV_{rdkt}^{-\phi} \cdot |\mathcal{R}_{dkt}|^{\rho} \cdot \varepsilon_{rdkt},$$

$$\frac{\partial C_{rdkt}}{\partial CV_{rdkt}} = w_k \cdot (-\phi) \cdot \left(f_{rdkt} \cdot \frac{L_r^T}{s_{rt}} \right)^{\gamma} \cdot CV_{rdkt}^{(\phi+1)} \cdot |\mathcal{R}_{dkt}|^{\rho} \cdot \varepsilon_{rdkt},$$

Taking logs,

$$\log(MC_{rdkt}^{CV}) = \log(w_k) + \gamma \log(f_{rdkt}) + \gamma \log\left(\frac{L_r^T}{s_{rt}} \right) - (\phi + 1) \log(CV_{rdkt}) + \rho \log(|\mathcal{R}_{dkt}|) + \log(\varepsilon_{rdkt})$$

$$\log(MC_{rdkt}^{f}) = \log(w_k) + (\gamma - 1) \log(f_{rdkt}) + \gamma \log\left(\frac{L_r^T}{s_{rt}} \right) - \phi \log(CV_{rdkt}) + \rho \log(|\mathcal{R}_{dkt}|) + \log(\varepsilon_{rdkt})$$

Econometric Specification I decompose the shock as

$$\log(\varepsilon_{rdkt}) = \alpha_k + \beta_d + \eta_r + u_{rdkt},$$

where α_k, β_d, and η_r are firm, depot, and route fixed effects, respectively. Substituting into the log marginal cost expressions yields the estimating equations:

$$\log(MC_{rdkt}^{f}) = (\gamma - 1) \log(f_{rdkt}) + \gamma \log\left(\frac{L_r^T}{s_{rt}} \right) - \phi \log(CV_{rdkt}) + \rho \log(|\mathcal{R}_{dkt}|) + \alpha_k + \beta_d + \eta_r + u_{rdkt},$$

$$\log(MC_{rdkt}^{CV}) = \gamma \log(f_{rdkt}) + \gamma \log\left(\frac{L_r^T}{s_{rt}} \right) - (\phi + 1) \log(CV_{rdkt}) + \rho \log(|\mathcal{R}_{dkt}|) + \alpha_k + \beta_d + \eta_r + u_{rdkt}.$$

GMM Estimation Let $\theta = (\gamma, \phi, \rho)$. After estimating and removing the fixed effects, I obtain residuals $\tilde{u}_{rdkt}^{f}$ and $\tilde{u}_{rdkt}^{CV}$, which enter the moment conditions. The GMM estimator solves

$$\hat{\theta}_{GMM} = \arg\min_{\theta} \left[\frac{1}{N} \sum_{n=1}^{N} g_n(\theta) \right]' W \left[\frac{1}{N} \sum_{n=1}^{N} g_n(\theta) \right],$$

where $g_n(\theta)$ collects the orthogonality conditions and W is a weighting matrix.

Moment Conditions and Instruments The moment conditions are

$$\mathbb{E}\left[Z^{f}_{rdkt} \cdot \tilde{u}^{f}_{rdkt}\right] = 0, \quad \mathbb{E}\left[Z^{CV}_{rdkt} \cdot \tilde{u}^{f}_{rdkt}\right] = 0, \quad \mathbb{E}\left[Z^{scale}_{dkt} \cdot \tilde{u}^{f}_{rdkt}\right] = 0, \quad \mathbb{E}\left[Z^{s}_{rdkt} \cdot \tilde{u}^{f}_{rdkt}\right] = 0,$$
$$\mathbb{E}\left[Z^{f}_{rdkt} \cdot \tilde{u}^{CV}_{rdkt}\right] = 0, \quad \mathbb{E}\left[Z^{CV}_{rdkt} \cdot \tilde{u}^{CV}_{rdkt}\right] = 0, \quad \mathbb{E}\left[Z^{scale}_{dkt} \cdot \tilde{u}^{CV}_{rdkt}\right] = 0, \quad \mathbb{E}\left[Z^{s}_{rdkt} \cdot \tilde{u}^{CV}_{rdkt}\right] = 0.$$

I use four sources of exogenous variation:

- Z^{f}_{rdkt}: disruptions such as burned or hijacked buses, which generate unexpected variation in realized f_{rdkt}.
- Z^{CV}_{rdkt}: changes in monitoring intensity around contract renewal as a shifter of CV_{rdkt}.
- Z^{scale}_{dkt}: reallocation of routes across depots following the rebundling reform, which generates variation in $|\mathcal{R}_{dkt}|$.
- Z^{s}_{rdkt}: free-flow nighttime speeds as a shifter of s_{rt}, isolating variation in average operating speed unrelated to traffic conditions during peak operations.

Together, these instruments generate exogenous variation in cost drivers, allowing me to trace out the marginal cost responses required to estimate $\theta = (\gamma, \phi, \rho)$.

Appendix C Figures and Tables (For Online Publication)

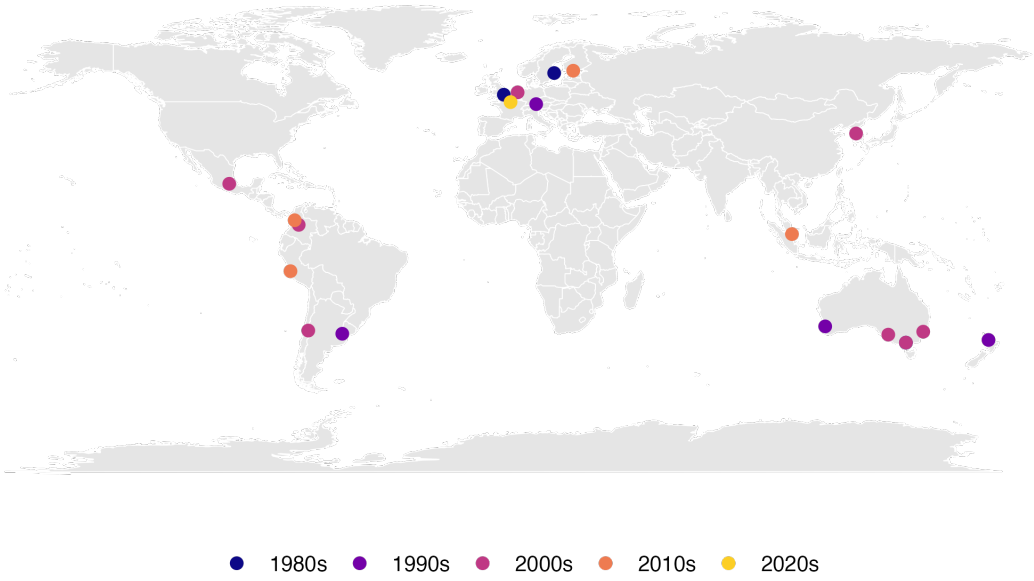

Figure C.1: Geographic distribution of cities adopting competitive tendering for public transit, by decade.

Table C.1: Mode Choice Summary Statistics

	N	Mean	SD
Panel A: Household Characteristics			
Household size	11,612	3.40	1.56
Vehicle ownership	11,612	0.47	0.50
Household number of vehicles	11,612	0.58	0.73
Income: $<$ USD 10k	11,612	0.31	0.46
Income: [USD 10k, 40k)	11,612	0.60	0.49
Income: $>$ USD 40k	11,612	0.09	0.28
Panel B: Traveler Characteristics			
Age (in years)	22,653	38.39	20.39
Female (= 1)	22,653	0.52	0.50
Education: Less than High School	22,653	0.24	0.42
Education: High School	22,653	0.43	0.49
Education: Associate degree	22,653	0.09	0.29
Education: College degree or higher	22,653	0.25	0.43
Panel C: Trip Characteristics			
Car available (= 1)	47,622	0.44	0.50
Origin within CBD (= 1)	47,622	0.31	0.46
Destination within CBD (= 1)	47,622	0.31	0.46
Driving (= 1)	47,622	0.39	0.49
Public Transit (= 1)	47,622	0.37	0.48
Walking (= 1)	47,622	0.25	0.43
Distance: [0 km, 2 km)	47,622	0.39	0.49
Distance: [2 km, 5 km)	47,622	0.23	0.42
Distance: $>$ 5 km	47,622	0.38	0.48
Purpose: Work	47,622	0.32	0.47
Purpose: Study	47,622	0.15	0.36
Purpose: Other	47,622	0.53	0.50

Notes: This table presents summary statistics for transportation mode choice decisions. Sample includes all observations from the travel preference parameters estimation sample covering the period 2012-2013. All monetary values are in 2013 USD.

Figure C.2: Example of a Bus Depot in Santiago's Public Transit System.

Notes: This photo shows the Rinconada depot, one of the largest operating facilities in Santiago's public transit system. Depots serve as the operational base for each firm. They house the fleet, provide charging and maintenance infrastructure, and include designated parking and dispatch lanes. All buses begin and end their daily operations at a depot, and depot–route assignments determine the pool of vehicles and personnel available for each route. *Source:* ATON.

Table C.2: Route Choice Summary Statistics

	Direct		Transfer	
	Mean	SD	Mean	SD
Panel A: Off-peak				
Number of options	3.13	3.07	5.38	6.95
At least one option (= 1)	0.83	0.37	0.73	0.45
Subway (= 1)	0.11	0.31	0.43	0.49
Fare (USD)	1.10	0.30	1.11	0.31
Travel time (min)	12.97	11.05	19.72	13.21
Wait time (min)	3.93	1.01	7.57	1.46
Panel B: Peak				
Number of options	2.34	2.47	4.31	6.06
At least one option (= 1)	0.77	0.42	0.66	0.47
Subway (= 1)	0.12	0.32	0.46	0.50
Fare (USD)	1.09	0.33	1.15	0.34
Travel time (min)	16.08	13.07	27.06	14.56
Wait time (min)	3.61	1.10	7.01	1.61

Notes: This table presents summary statistics for route choice decisions. Sample includes all observations from travel preference parameters estimation sample covering the period 2012-2013. All monetary values are in 2013 USD.

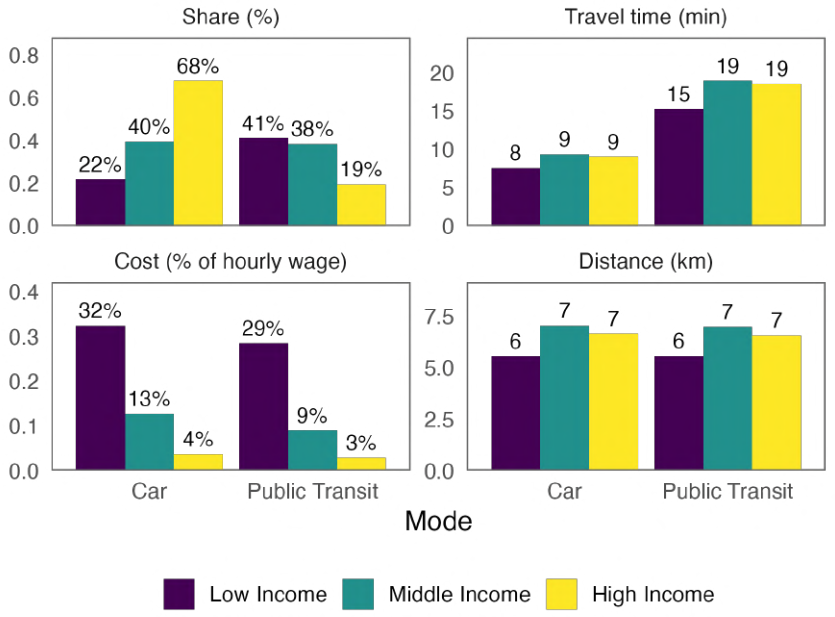

Figure C.3: Variation in Mode Choice Attributes across Income Groups.

Notes: The figure displays variation in mode choice attributes across income groups, showing mode share, travel time, cost (as a percentage of the hourly wage), and distance for car users and public transit users. The displayed shares cover only car and public transit, with walking treated as the outside option to bring total mode shares to 100%.

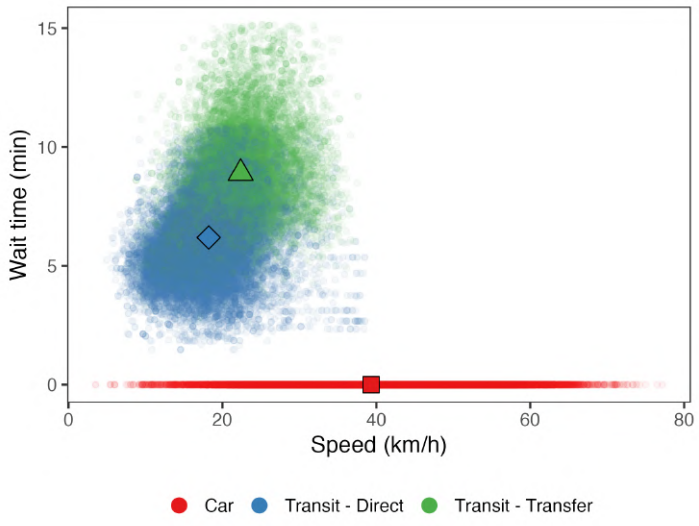

Figure C.4: Speed-Wait Time Trade-offs in Route Choice.

Notes: The figure illustrates the speed-frequency trade-off in route choice, plotting frequency-implied wait times against travel speeds. The scatter plot reveals distinct clusters for different route types: cars, direct transit routes, and transfer-based transit options. Squared, Triangular and diamond markers indicate mean values for different route categories.

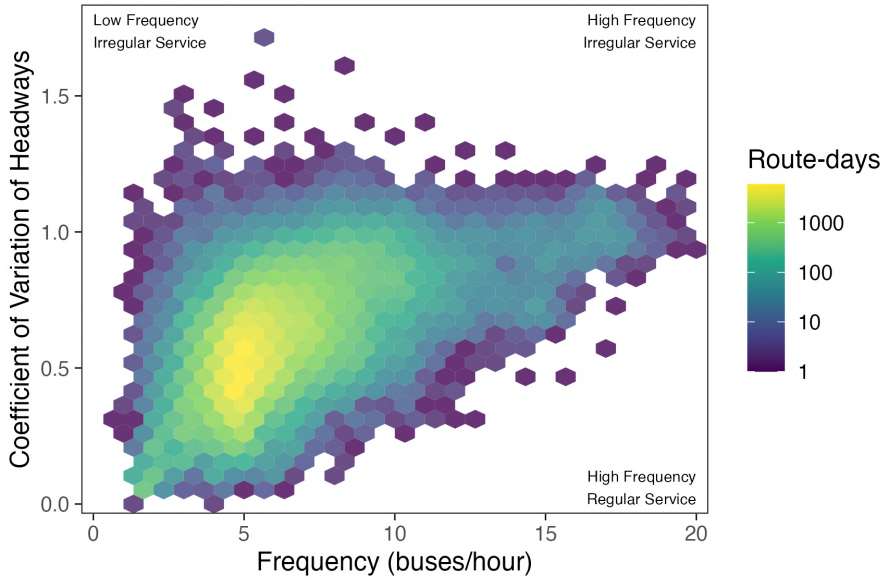

Figure C.5: Frequency and Headway Regularity Choice Patterns.

Notes: The figure shows the distribution of route-day observations according to service frequency and headway regularity. Frequency is expressed in buses per hour. Regularity is measured with the coefficient of variation of headways. Color intensity reflects the density of observations in each region of the plot.

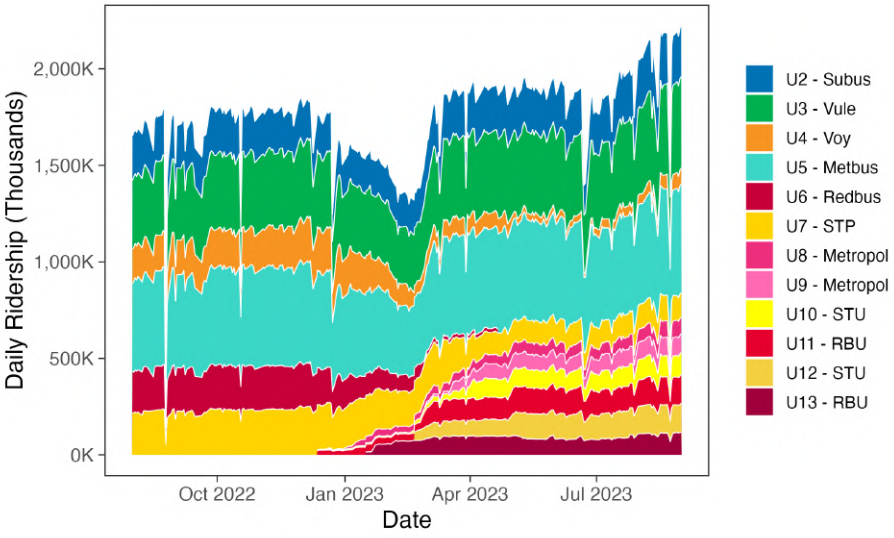

Figure C.6: Firm Level Ridership Market Share.

Notes: The figure displays daily ridership trends across transit firms from August 2022 to August 2023, with each colored area representing a different operator's passenger volume. The stacked area chart shows bus system ridership fluctuating between approximately 1.6-2.2 million daily passengers.

Table C.3: Public Transit Supply Summary Statistics

	Mean	SD	Min	Max
Panel A: System-level				
Number of Bundles	8.50	2.53	6.00	11.00
Number of Firms	7.00	1.01	6.00	8.00
Number of Depots	65.84	2.05	62.00	68.00
Number of Routes	354.86	10.86	295.00	363.00
Daily Ridership (millions)	1.86	0.32	0.43	2.21
Panel B: Bundle-level				
Number of Depots	8.10	6.03	2.00	19.00
Number of Routes	41.75	23.67	11.00	89.00
Daily Ridership (thousands)	218.72	145.45	49.48	562.91
Panel C: Route-level				
Frequency (bus/h)	5.82	1.96	1.06	20.27
Headway Regularity (CV)	0.41	0.15	0.02	1.42
Length (km)	18.45	8.58	2.35	57.22
Speed (km/h)	17.83	3.32	1.44	39.29
Daily Ridership (hundreds)	28.52	24.72	0.01	170.64

Notes: This table presents summary statistics for public transit supply characteristics across three levels of aggregation. The sample includes route-day level observations from August 2022 and August 2023 to capture initial and final equilibrium states, excluding transient periods. Panel A shows system-level statistics aggregated across all bundles and routes. Panel B presents bundle-level statistics, where bundles represent groups of routes operated under the same contract. Panel C displays route-level characteristics including service frequency (buses per hour), headway regularity measured by coefficient of variation (CV), route length, average speed, and ridership.

(a) Physical Road Network and Traffic Sensors

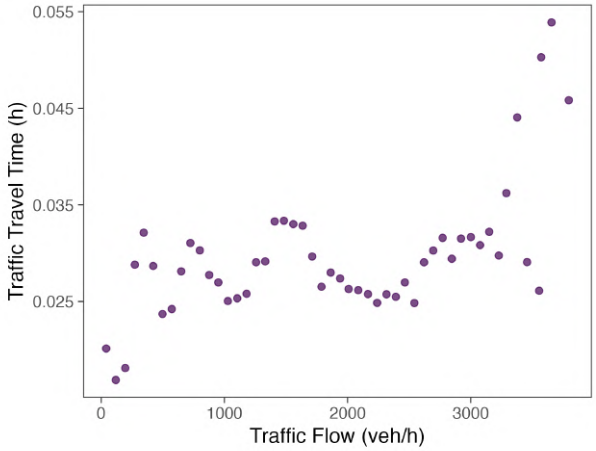

(b) Traffic Flow vs. Travel Time

Figure C.7: Traffic Flow and Traffic Speed

Notes: Panel (a) displays the physical road network, with street centerlines in black and traffic sensors in red that record vehicle flows every 15 minutes. Panel (b) illustrates the traffic flow-travel time relationship. The gray points represent individual observations, while the purple line shows the binned averages.

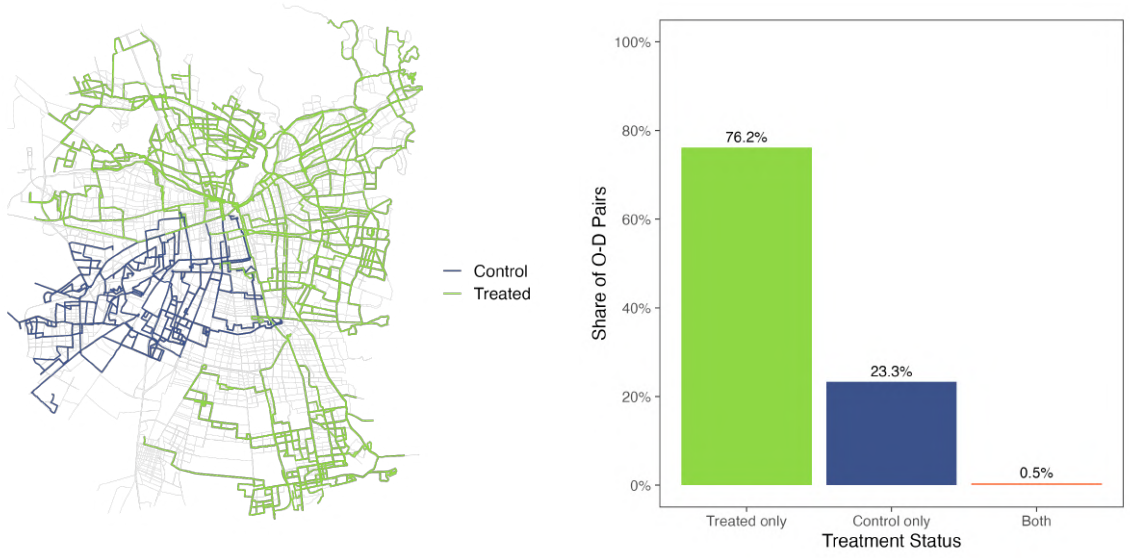

(a) Treated vs Control Routes

(b) Share of O-D pairs by treatment group

Figure C.8: Quality Targets Treatment Assignment and Overlap in Transit Travel Options.

Notes: The figure shows the spatial distribution of treated and control transit routes and the composition of origin–destination (O–D) pairs across treatment groups. Panel (a) displays the route network, where treated routes are shown in green and control routes are shown in blue. Panel (b) shows the share of O–D pairs whose available transit options include only treated routes, only control routes, or a mix of both. The sample of O–D pairs is restricted to those that include at least one treated or control route as the first leg of a feasible transit option; O–D pairs served only by routes outside these groups are excluded.

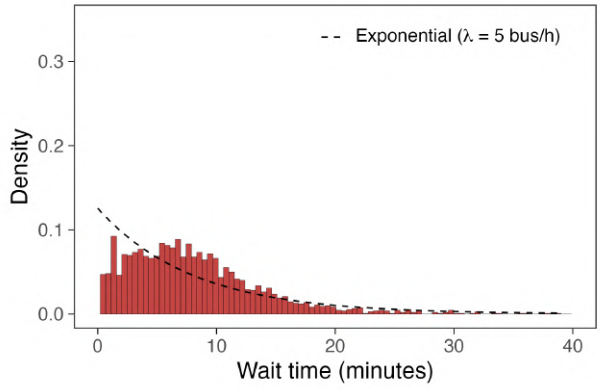

(a) Frequency = 5 bus/h

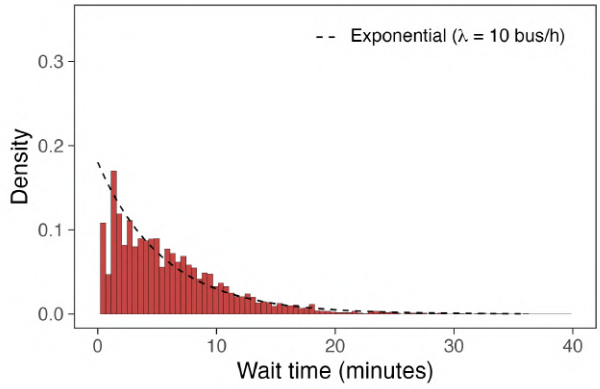

(b) Frequency = 10 bus/h

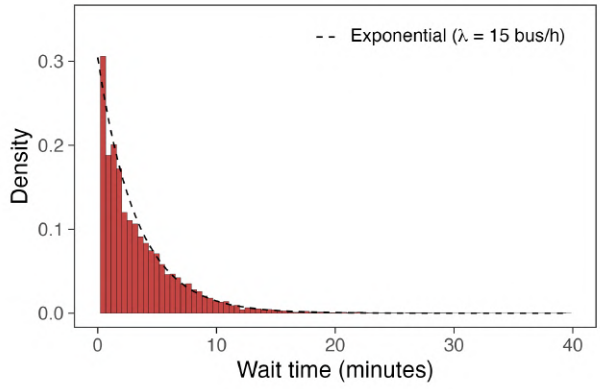

(c) Frequency = 15 bus/h

Figure C.9: Wait Time Distribution by Service Frequency Level.

Notes: The figure shows the empirical distribution of traveler wait times for a representative bus route operating at a given frequency. Panel (a) corresponds to a route with 5 buses per hour, Panel (b) to a route with 10 buses per hour, and Panel (c) to a route with 15 buses per hour. Bars show the empirical distribution of passenger wait times computed from GPS-based headway data, while the dashed line depicts the exponential distribution predicted under a Poisson bus arrival process with rate parameter λ equal to the observed average service frequency.

Figure C.10: Topological Representation of the Road Network in Santiago, Chile.

Notes: This figure shows the topological representation of Santiago's road network, where bus stations serve as nodes (light blue) and edges (gray) represent the fictitious connections between adjacent stations in the graph.